AD-A121 297   RADAR ANALYSIS FOR SEVERE WEATHER DETECTION AND   1/1
TRACKING(U) ENVIRONMENTAL RESEARCH AND TECHNOLOGY INC
CONCORD MA R K CRANE JUL 82 ERT-P-A579-F
UNCLASSIFIED DOT/FAA/RD-82/64 DTFA01-81-Y-10521   F/G 17/9   NL

END
FILMED
DTIC

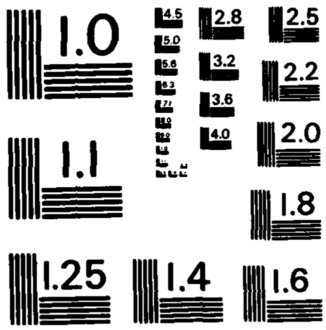
1.0
4.5
5.0
5.6
6.3
2.8
3.2
3.6
4.0
2.5
2.2
2.0
1.1
1.8
1.25
1.4
1.6

AD A121297

DOT/FAA/RD-82/64

Systems Research &
Development Service
Washington, D.C. 20591

Radar Analysis for Severe Weather Detection and Tracking

R. K. Crane

July 1982

Final Report

This document is available to the U.S. public through the National Technical Information Service, Springfield, Virginia 22161.

U.S. Department of Transportation
Federal Aviation Administration

NOTICE

Technical Report Documentation Page

1. Report No.	2. Government Accession No.	3. Recipient's Catalog No.
DOT/FAA/RD-82/64	AD-A121297	

4. Title and Subtitle	5. Report Date
Radar Analysis for Severe Weather Detection and Tracking	July 1982
	6. Performing Organization Code P-A579
7. Author(s) Robert K. Crane	8. Performing Organization Report No. P-A579-F
9. Performing Organization Name and Address Environmental Research & Technology, Inc. 696 Virginia Road Concord, Massachusetts 01742	10. Work Unit No. (TRAIS) 156-410-01W 11. Contract or Grant No. NA80RAC00110
12. Sponsoring Agency Name and Address U. S. Department of Transportation Federal Aviation Administration Systems Research and Development Service Washington, D. C. 20591	13. Type of Report and Period Covered Final Report July 1980 - June 1981 14. Sponsoring Agency Code FAA/ARD-410

15. Supplementary Notes

Prepared under sections of FAA Interagency Agreement No. DTFA01-81-Y-10521, managed by the Aviation Weather Branch ARD-410 and National Severe Storms Lab., NOAA, 1313 Halley Circle, Norman, OK 73069.

16. Abstract

The cell detection and tracking algorithms, were refined to incorporate Doppler radar derived estimates of tangential shear in the tracking process without significantly increasing the tracking error and the number of detected cell clusters. The Doppler data were subjected to a number of processing steps designed to minimize the false cell and cluster problem (false alarm rate). The revised thunderstorm hazard detection algorithm employs spatially filtered tangential shear data with a 10 dB minimum signal-to-noise ratio. Shear cell continuity in time is required to establish a volume cell in the absence of a reflectivity cell.

National Severe Storms Laboratory Doppler radar data were analyzed to evaluate the refined algorithms. Tangential shear and Doppler spread (spectrum width) data were used separately for the detection of potentially hazardous regions. Intercomparison between isolated volume cells simultaneously detected by the Norman and Cimarron radars showed that both the shear and spread observations were aspect sensitive (anisotropic). The incorporation of Doppler (shear) data produced more than twice the number of volume cells, only slightly increased the number of clusters, and only slightly increased the rms tracking error. The Doppler data were used to develop an augmented set of attributes potentially useful for hazard detection.

17. Key Words	18. Distribution Statement
Thunderstorm turbulence, Doppler radar, cell tracking, storm detection, weather radar data processing	Document is available to the U.S. public through the National Technical Information Service, Springfield, Virginia 22151.

19. Security Classif. (of this report)	20. Security Classif. (of this page)	21. No. of Pages	22. Price
Unclassified	Unclassified	91	

METRIC CONVERSION FACTORS

Approximate Conversions to Metric Measures

Symbol	When You Know	Multiply by	To Find	Symbol
		LENGTH		
in	inches	*2.5	centimeters	cm
ft	feet	30	centimeters	cm
yd	yards	0.9	meters	m
mi	miles	1.6	kilometers	km
		AREA		
in^2	square inches	6.5	square centimeters	cm^2
ft^2	square feet	0.09	square meters	m^2
yd^2	square yards	0.8	square meters	m^2
mi^2	square miles	2.6	square kilometers	km^2
	acres	0.4	hectares	ha
		MASS (weight)		
oz	ounces	28	grams	g
lb	pounds	0.45	kilograms	kg
	short tons (2000 lb)	0.9	tonnes	t
		VOLUME		
tsp	teaspoons	5	milliliters	ml
Tbsp	tablespoons	15	milliliters	ml
fl oz	fluid ounces	30	milliliters	ml
c	cups	0.24	liters	l
pt	pints	0.47	liters	l
qt	quarts	0.95	liters	l
gal	gallons	3.8	liters	l
ft^3	cubic feet	0.03	cubic meters	m^3
yd^3	cubic yards	0.76	cubic meters	m^3
		TEMPERATURE (exact)		
°F	Fahrenheit temperature	5/9 (after subtracting 32)	Celsius temperature	°C

*1 in = 2.54 (exactly). For other exact conversions and more detailed tables, see NBS Misc. Publ. 286, Units of Weights and Measures, Price $2.25, SD Catalog No. C13.10:286.

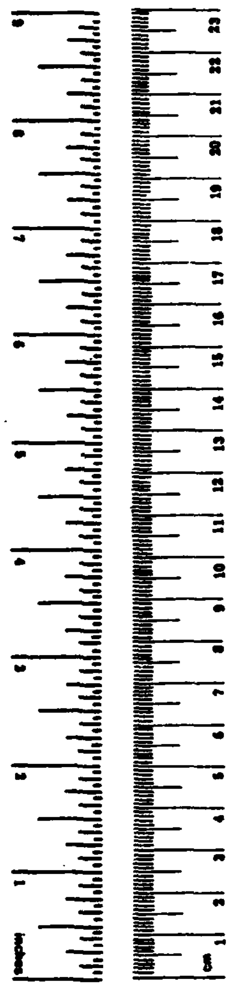

Approximate Conversions from Metric Measures

Symbol	When You Know	Multiply by	To Find	Symbol
		LENGTH		
mm	millimeters	0.04	inches	in
cm	centimeters	0.4	inches	in
m	meters	3.3	feet	ft
m	meters	1.1	yards	yd
km	kilometers	0.6	miles	mi
		AREA		
cm^2	square centimeters	0.16	square inches	in^2
m^2	square meters	1.2	square yards	yd^2
km^2	square kilometers	0.4	square miles	mi^2
ha	hectares (10,000 m^2)	2.5	acres	
		MASS (weight)		
g	grams	0.035	ounces	oz
kg	kilograms	2.2	pounds	lb
t	tonnes (1000 kg)	1.1	short tons	
		VOLUME		
ml	milliliters	0.03	fluid ounces	fl oz
l	liters	2.1	pints	pt
l	liters	1.06	quarts	qt
l	liters	0.26	gallons	gal
m^3	cubic meters	35	cubic feet	ft^3
m^3	cubic meters	1.3	cubic yards	yd^3
		TEMPERATURE (exact)		
°C	Celsius temperature	9/5 (then add 32)	Fahrenheit temperature	°F

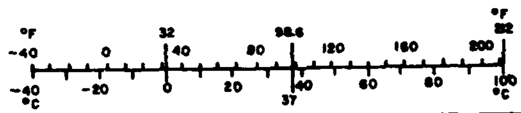

ACKNOWLEDGEMENTS

The study reported in this document was funded by the Federal Aviation Administration under an interagency agreement with the National Oceanic and Atmospheric Administration, Environmental Research Laboratories, National Severe Storms Laboratory via a contract with the Environmental Research and Technology, Inc.

The author wishes to acknowledge the support of F. Coons and F. Melewicz of the FAA/Aviation Weather Branch and of J. Lee and K. Wilk of the National Severe Storms Laboratory. J. Hinkelman (now with the NOAA, PROFS program) was a strong supporter of the work and instrumental in initiating the program.

Special thanks goes to Ken Hardy for his supervision and guidance while manager of the Earth Resources and Atmospheric Physics Division at ERT. The work of Gary Gustafson while he was a programmer at ERT was critical to the success of the program.

The computer processing required for program development and test was performed on the FAA supported VAX 11/780 computer at the MITRE Corporation, McLean, Virginia. Art McClinton of the MITRE Corporation provided the support and advice required to make the long distance computer processing successful.

TABLE OF CONTENTS

Page

1. INTRODUCTION 1

   1.1 Program Objectives 1

   1.2 Summary of Results 2

   1.3 Air Traffic Control Applications 6

   1.4 Organization of the Report 8

2. BACKGROUND 10

   2.1 Summary of Prior Work at Environmental Research & Technology, Inc. (ERT) 10

   2.2 Rationale for Algorithm Revision 14

3. THE FALSE ALARM PROBLEM 17

   3.1 Use of Tangential Shear for Velocity Perturbation Detection 17

      3.1.1 Statistical Properties of Pulse Pair Estimates 17

      3.1.2 Relationship between Spread and Shear in a Turbulent Region 21

      3.1.3 Relative Merits of Spread and Shear Estimates 26

   3.2 Requirement for Spatial Filtering 33

4. ALGORITHM REFINEMENT 40

   4.1 Preprocessing 40

   4.2 Tracking 42

   4.3 Graphical Display 44

5. ANALYSIS OF NATIONAL SEVERE STORMS LABORATORY (NSSL) DATA 45

   5.1 Intercomparison of Cimarron and Norman Radar Cell Detection Data 45

   5.2 Tracking Analysis 51

TABLE OF CONTENTS (cont.)

		Page
6.	USE OF WSR-57 RADARS FOR HAZARD DETECTION	69
7.	INCORPORATION OF SATELLITE IMAGERY	74
8.	CONCLUSIONS AND RECOMMENDATIONS	78
9.	REFERENCES	81

LIST OF ILLUSTRATIONS

Figure #	Caption	Page
1	Display output from the cell detection and tracking program. Norman radar data, 1031 CST, June 19, 1979. The contoured echo boundary is for a reflectivity of 20 dBZ, the volume cells are marked by +, the centroid locations of clusters by x, and, for clusters with a minimum 3 scan lifetime, a 1.4 h extrapolation along the smoothed track motion vector is depicted by a dashed line.	7
2	Performance of contiguous pulse pair and independent pulse pair estimators of the Doppler velocity.	19
3	Doppler spread (spectrum width) estimation bias.	22
4	Performance of contiguous pulse pair and independent pulse pair estimators of the Doppler spread (spectrum width).	23
5	Relative performance of Doppler spread (spectrum width) and tangential shear estimators when the true spectrum width is produced by a vertical shear of 3.2 m/s/km. Results for 64 independent pulse pairs.	29
6	Relative performance of Doppler spread (spectrum width) and tangential shear estimators when the true spectrum width is produced by a vertical shear of 3.2 m/s/km. Results for 64 contiguous pulse pairs.	30
7	Relative performance of Doppler spread (spectrum width) and tangential shear estimators when the true spectrum width is produced by a horizontal shear of 3.2 m/s/km. Results for 64 contiguous pulse pairs.	32
8	Intercomparison between simultaneous reflectivity measurements using isolated volume cells.	47

LIST OF ILLUSTRATIONS (cont.)

Figure #	Caption	Page
9	Intercomparison between simultaneous tangential shear measurements using isolated volume cells.	48
10	Intercomparison between simultaneous Doppler spread (spectral width) measurements using isolated volume cells.	50
11	Intercomparison between tangential shear and radial shear measures of velocity perturbation for the same isolated volume cells.	52
12	Summary parameters for the June 16, 1980 observation set. Both echo area and the water flux (area integrated rain rate) are displayed.	54
13	Counts of the numbers of active volume cells and clusters for four separate tracking runs.	55
14	Average tracking velocities for the separate tracking runs.	56
15	RMS tracking errors for the separate tracking runs.	58
16	Number of volume cells employed for tracking in each of the tracking runs.	59
17	Rotation estimates for clusters based on tracking data.	64
18	Divergence estimates for clusters based on tracking data.	65
19	Comparison between rotation estimates and divergence estimates for identical data with different initial track velocity estimates.	66
20	Comparison between rotation estimates and divergence estimates for the same clusters as detected using reflectivity data only or using reflectivity plus tangential shear data.	67

LIST OF ILLUSTRATIONS (cont.)

Figure #	Caption	Page
21	Relative detection frequencies for volume cells and cluster derived from the entire Kansas data set (Crane and Hardy, 1981, Figures 4-6) and from the JDOP data set (JDOP, 1979).	71

1. INTRODUCTION

1.1 Program Objectives

The timely detection and short range forecast of regions of convective storms which are hazardous to aircraft operations are of vital importance to the safety of flight and the efficient management of the nation's airspace. Weather radars have the capacity to observe the fine structure of severe weather and to localize regions of potential hazard.

Single Doppler radars can be used to detect the perturbations in the wind field associated with hazardous conditions. The velocity perturbations can be detected by observing a component of the shear (Wilson *et al.*, 1980; Crane, 1981) or the velocity variance (Lee, 1977). Studies comparing aircraft and radar observations have shown that high hazard detection probabilities can be obtained using either the shear or variance data from the radar but that high false alarm rates are also obtained. The objective of this research rogram is the development of hazard detection algorithms which maintain a high detection probability while minimizing the false alarm rate.

Specifically, the research program is to:

1. continue the development of algorithms for estimating the intensity of turbulence and predicting the development and motion of regions hazardous to aircraft using both conventional

and Doppler radar data;

2. develop a non-real-time demonstration of the use of the National Severe Storms Laboratory (NSSL) conventional WSR-57 weather radar for hazard detection.

3. provide consultation on weather radar system design for Federal Aviation Administration (FAA) applications;

4. consider the integration of satellite IR data into the detection and tracking algorithms; and

5. participate in the development of a real-time capability for demonstration of the detection and tracking algorithms using conventional weather radar data [as directed by the FAA].

1.2 Summary of Results

The research effort concentrated on item (1) of the list of specific objectives, continued algorithm development. Consultation on weather radar system design was provided to the FAA as requested (item 3) and will not be considered further in this report. The FAA did not have suitable facilities for a real-time demonstration of the detection and tracking algorithms and, at the direction of the FAA, no effort was made on item (5).

Data from the 1980 field season at the National Severe Storms Laboratory (NSSL) was to be used for algorithm development (item 1) and the non-real-time demonstration of the use of the WSR-57 for hazard detection (item 2). Unfortunately, the thunderstorm activity at NSSL was below normal in 1980 (Lee and Doviak, 1981) and data from only one storm were provided for

analysis. The data were not adequate for the demonstration of the use of WSR-57 data for hazard detection (item 2). Data from the Kansas HIPLEX program (Crane and Hardy, 1981) and from the earlier analysis of the National Hail Research Experiment (NHRE) data for the evaluation of the cell algorithms for hazard detection (Crane, 1981) were employed, instead, to evaluate the utility of WSR-57 data for hazard detection.

The earlier NHRE data analysis showed that for radar ranges between 40 and 80 km, the 1° beamwidth, S-band, CP-2 (conventional) radar was competitive with the C-band and X-band Doppler radars for the detection of moderate or more intense turbulence. The detection probability was greater than 0.75 for a 4 km radius of influence about a cell for the conventional (reflectivity only) radar but less than 0.7 for the Doppler radars and the same radius of influence. The false alarm rates were similar for the different types of radars, less than 0.15.

The WSR-57 conventional weather radar has a large equivalent beamwidth. The elevation and azimuth beamwidths of the WSR-57 are more than twice the beamwidth of the S-band, CP-2 radar. An earlier analysis of the Kansas HIPLEX data revealed that the detection probability for a cluster (or velocity perturbation) was cross-beam resolution dependent where the cross-beam resolution (distance) of a radar system is given by the range, beamwidth product at the observation range. Based on the results of the Kansas study, the detection

probability of the conventional WSR-57 radar should be only 43 percent of the detection probability of the CP-2 radar at the same range. That is, the WSR-57 could perform as well as the CP-2 radar at half the range but, at the ranges employed in the NHRE penetration study, the detection probability would be significantly poorer, less than .32.

The NHRE penetration study showed that the cluster detection algorithms provided high detection probabilities when used with conventional or with Doppler data. Although more information about the storm should be available in the Doppler data, it was not used effectively by the cluster detection algorithm. In the final report on the NHRE penetration study (Crane, 1981) a number of recommendations were made to use more effectively Doppler data in the detection algorithm. These recommendations were incorporated in the processing program as a part of the continued refinement of the algorithms (item 1). The program was also rewritten for use on the Digital Equipment Corporation (DEC) VAX-11/780 computer operated for the FAA by the MITRE Corporation in McLean, Virginia and revised to accept data from the NSSL radars. The report "Detection and Tracking Algorithm Refinement" by Gustafson and Crane (1981) documents the new program.

The algorithm refinements were made with the NHRE data analysis problems in mind. The high false shear-cell alarm rate was reduced by signal-to-noise dependent thresholding of data for processing, by the incorporation of spatial filtering in the

data preparation algorithms and by associating velocity perturbation cells with reflectivity cells in the tracking algorithms. The program was also revised to use either tangential shear, radial shear, total shear, or range normalized Doppler spread for the detection of a velocity perturbation. The radial velocity variation with height within a volume cell was also calculated for use in characterizing a vertical shear or, for the most intense cells, to detect a blocking cell. A number of additional refinements were made to accommodate the widely spaced (in elevation) sector scans employed by NSSL and to accommodate the dual pulse repetition frequency (prf) of the NSSL radar.

An evaluation of the algorithm refinements for turbulence hazard detection could not be made because of the lack of observations. Data from the Joint Airport Weather Studies (JAWS) program (NCAR, 1982) should be used for such an evaluation. Available data were studied to deduce the possible effect of the algorithm revisions. As the result of this study, the use of spatially filtered tangential shear data is recommended for the detection of velocity perturbations.

Severe turbulence was observed to occur in the low reflectivity regions ahead of a storm where new cell development will take place (Crane, 1981). Neither conventional nor Doppler weather radar observations are useful for the detection of turbulence in such regions and the existence of the hazard must be inferred from the structure of the available radar data and,

perhaps, from the incorporation of additional data from the visible and infrared frequency scanning radiometers on geostationary satellites. A study was made to show that the incorporation of satellite data was feasible (item 4) but, under this contract, no program modifications were made to accomplish the integration of satellite data into the tracking and hazard detection algorithms.

1.3 Air Traffic Control Applications

The ultimate goal of this research program is the development of an automated, real-time thunderstorm hazard detection and short range forecast system for use by enroute and terminal area air traffic controllers. Under this contract, the cell detection and tracking program was revised to use single Doppler radar data to provide reflectivity and spatially filtered velocity perturbation (shear) information for cell and cluster detection and tracking. Plotting routines were developed to prepare displays which show the current and projected locations of the volume cells and clusters (Figure 1). The volume cell identification algorithm was revised to provide information on volume cell age and association with developing convection. The program revisions were made to provide displays that could be readily interpreted to obtain the locations and to forecast movement of hazardous regions.

The development of an automated hazard detection system for the FAA is still incomplete. The algorithms produced under this contract still need to be tested. The test procedure

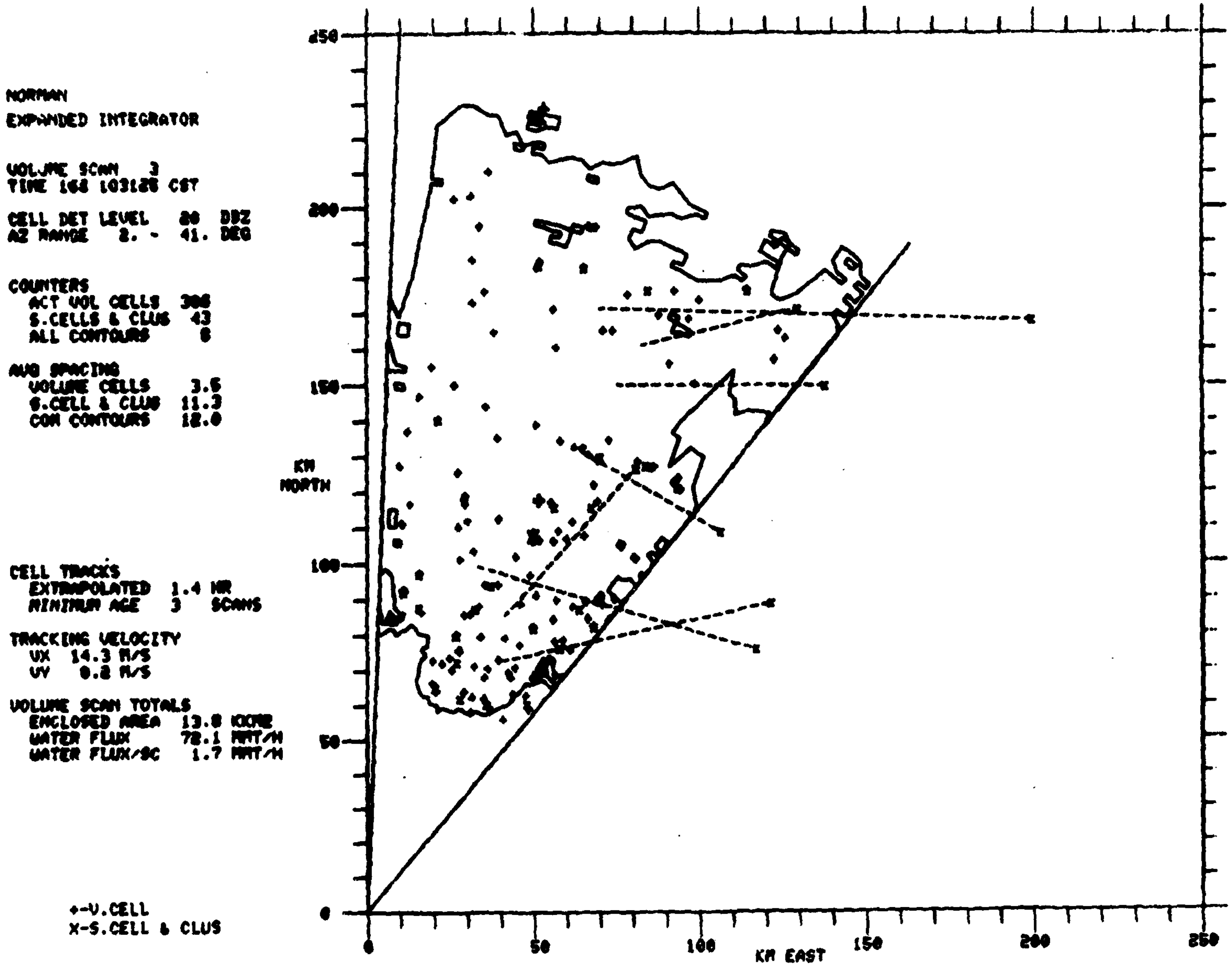

Figure 1. Display output from the cell detection and tracking program. Norman radar 1031 CST, June 19, 1979. The contoured echo boundary is for a reflectivity of 20 dBZ, the volume cells are marked by +, the centroid locations of clusters by x and, for clusters with a minimum 3 scan lifetime, a 1.4 h extrapolation along the smoothed track motion vector is depicted by a dashed line.

should explore both the detection problem and, more importantly, the false alarm problem. At the present time, only the data from the JAWS experiment are useful for such an undertaking.

The program has a number of constants and thresholds that are used in the tracking process and in the identification of hazardous regions. These constants and thresholds were set on the basis of an extremely limited set of data. Experience must be gained with the use of the program first in a research environment to set the constants and then in an operational environment to evaluate its performance. Much of the evaluation may be done in non-real-time but eventually a real-time test is required.

1.4 Organization of the Report

This report summarizes the results of the 1980-1981 research effort at Environmental Research & Technology, Inc. (ERT) during the time period July 1980 through June 1981. The work was conducted for the Federal Aviation Administration under an interagency agreement with the National Oceanic and Atmospheric Administration and contract with ERT. The major effort, the continued algorithm development, is described in Sections 2 through 5. Section 2 introduces the rationale for the algorithm revisions, Section 3 considers the false alarm rate and the use of shear or Doppler spread for the detection of

turbulence, Section 4 documents the algorithm revisions, and Section 5 reports on the analysis of the operation of the revised algorithms on a limited data set of NSSL. Section 6 discusses the utility of conventional WSR-57 radar data and Section 7 considers the incorporation of satellite data in the processing scheme. Finally, Section 8 summarizes the conclusions and provides recommendations for future work.

2. BACKGROUND

2.1 Summary of Prior Work at Environmental Research & Technology, Inc. (ERT)

The cell detection and tracking algorithms developed by ERT (Crane, 1979) were intended for the automatic, real-time detection of turbulent regions hazardous to aircraft penetration. ERT conducted an evaluation of the hazard detection scheme (Crane, 1981) using National Hail Research Experiment (NHRE) case study data and the South Dakota School of Mines and Technology (SDSMT) instrumented T-28 aircraft penetration flight data. The evaluation revealed:

1. the cell detection algorithm successfully extracted reflectivity and shear cells from the radar data fields;

2. the reflectivity and shear cell observations could be combined from different times, heights and radars to produce stable volume cell tracks;

3. the locations of significant volume cells or clusters derived from only the reflectivity data and the locations of aircraft encounters with turbulence were highly correlated;

4. the addition of Doppler (shear) information did not appreciably change the statistical relationship between volume cell occurrences and turbulence encounters;

5. the probability of detecting turbulence within

a radar echo region (reflectivity greater than 20 dBZ) was high, greater than .94;

6. the false alarm rate for turbulence detection was relatively high, especially if only the most intense turbulence encounters were to be detected, and

7. the correlations between any of the measures used for the intensity of a volume cell, reflectivity or shear magnitude, and the intensity of turbulence encountered by the aircraft was low.

The results of the previous study showed that turbulence could be detected successfully with a low false alarm rate if the level of turbulence to be detected was sufficiently low but the detection scheme did not work well if only the extreme levels of turbulence were of interest. Lee (1977,1981) similarly found a good correlation between the locations of turbulence and regions with a Doppler spread (square root of the velocity variance) in excess of 4 m/s but a poor correlation between the magnitude of the Doppler spread and the intensity of the turbulence. The observed correlation coefficients were equal to .4 for one year and to less than .2 for two other years. Lewis (1981) also reported poor correlations between the intensity of turbulence and the magnitude of the Doppler spread.

The results of simultaneous radar and aircraft observations of thunderstorm turbulence show that the occurrence of turbulence is strongly coupled with the occurrence of a detectable Doppler velocity field perturbation and that

either shear or spread measurements can be used to observe the velocity field perturbations. Crane (1981) went further to show that two major problems still exist, however, in attempting to use Doppler data for turbulence hazard detection, 1) the high false alarm rate that is obtained if only extreme levels of turbulence are of interest due to the poor correlation between the intensity of turbulence and the measure of the velocity perturbation and 2) the occurrence of significant turbulence outside the radar echo volume which cannot be detected by weather radar. He concluded that additional information must be extracted from the structure of the reflectivity and Doppler velocity fields to reduce the false alarm problem and that short range forecast procedures must be developed to address the problem of undetectable turbulence.

As a result of the prior ERT study, the following program was recommended:

"1. refine the cell and cluster detection algorithms to reduce the effect of the statistical uncertainties in the estimation of velocity perturbations;

2. refine the cell significance algorithms using cell age, location in the development pattern, apparent vertical transport of horizontal momentum and similar parameters to provide an indication of the intensity of the turbulence;

3. develop a graphical display of the cell, cluster, and contour data that can be provided both to meteorologists for the development of short range forecasts and to controllers for use in vectoring test aircraft into regions expected to be hazardous or free of hazard to evaluate the algorithms;

4. develop a real-time version of the program for use in the continued evaluation of the algorithms;

5. using the real-time system and controller displays, conduct flight tests to evaluate the refined velocity perturbation detection and turbulence intensity estimation algorithms;

6. analyze the new cell and cluster development patterns to isolate the propagating disturbances that trigger the convection;

7. automate the display of the propagating disturbances to provide forecasters and controllers with the tools necessary for the short range forecast of hazardous areas;

8. evaluate the short range hazardous region forecast procedures in several different climate regions, and

9. based on the short range hazard forecast evaluations, automate the successful features to provide timely forecasts to the controllers."

In the research program reported herein, items (1), (2) and (3) have been addressed.

2.2 Rationale for Algorithm Revision

Two problems were evident with the algorithm set used for the analysis of the NHRE case study data, (1) a tendency to produce a number of spurious shear cells, and (2) an inadequate measure of the intensity of turbulence to be associated with a shear cell or cluster of cells. The spurious cell problem appeared to be dependent on the signal-to-noise ratio and to require additional signal processing for its alleviation. The inadequate measure of turbulence is of a more fundamental nature and requires the extraction of more information from the structure and development of the complex of convective cells and clusters.

The conceptual model employed for the development of the turbulent hazard detection scheme (Crane, 1981, Section 2.2) envisioned two or more tangential shear cells in the near vicinity of each developing and potentially hazardous convective cell. Based on this model, a number of individual shear cells could be associated with a single volume cell. The algorithm used in the NHRE data analysis was developed for the analysis of reflectivity cells based on the assumption that each reflectivity cell should correspond to a volume cell and two or more volume cells in close proximity belong to a cluster. When used with tangential shear data, this algorithm produced far too many volume cells and clusters and, in the extreme, combined all the volume cells in an echo region

into one very large cluster (Crane, 1981, data for the NOAA-C radar in Figure 11 and 12). Three revisions to the processing algorithms were required to alleviate these problems, (1) signal-to-noise dependent processing thresholds to reduce the number of spurious shear cells, (2) spatial filtering to further reduce the number of spurious shear cells, and (3) the association of multiple shear cells with a single volume cell to reduce the number of spurious volume cells and clusters.

The revisions required to provide a more meaningful measure of turbulence intensity were not as obvious and may still require further revision. The results of the NHRE case study data analysis showed that the tangential shear magnitudes (and, by induction, the Doppler spread) were aspect sensitive (Crane, 1981, Figures 17, 19 and 20). This was argued to be expected because the cross-beam resolution (range, beamwidth product) was larger than the outer scale for the turbulence. Because of the aspect sensitivity the same velocity perturbation should produce different shear (or spread) values depending upon the location of the radar relative to the location of the perturbation. If multiple radars were used, the largest observed shear magnitude value may provide a good estimate of the intensity of the hazard but, with data from only a single Doppler radar, additional information is necessary to provide an estimate of the magnitude of the hazard. The prior study concluded (item 2 above)

that cell age, location in the development pattern, and a measure of the variation of horizontal momentum with height within a cell may provide the required additional information.

3. THE FALSE ALARM PROBLEM

3.1 Use of Tangential Shear for Velocity Perturbation Detection

Studies of the use of Doppler radars for the detection of turbulence hazardous to aircraft safety have employed either Doppler spread (Lee, 1977; Lewis, 1981) or Doppler velocity shear (Crane, 1981) measurements with equal success. Crane, however, has pointed out the importance of the false alarm problem in turbulence detection and has recommended the use of shear instead of spread observations as a way of reducing that problem. The case for the use of shear instead of spread rests on (1) the differences in the signal statistics from a pulse pair processor as a function of the signal-to-noise ratio and (2) on the intimate relationship between shear and turbulence in the three dimensional flow field of a convective storm.

3.1.1 Statistical Properties of Pulse Pair Estimates - The estimation uncertainties for pulse pair observations of the Doppler spread and Doppler velocity have been analyzed by Miller and Rochwarger (1972) for the case of uncorrelated pulse pairs and by Berger and Groginsky (1973) and by Zrnić (1977) for correlated pulse pairs. Zrnic showed that independent, spaced, and contiguous pulse pair estimators produce comparable results at high signal-to-noise ratios when observations are obtained over the same interval and comparable results at low signal-to-noise ratios when the same number of pulses are used. At low signal-to-noise ratios the contiguous pair estimator

performs marginally better than the independent pair estimator for the estimation of Doppler velocity but the independent pair estimator performs better for the estimation of Doppler (spectrum width) spread. In this report, the results of analyses for both independent pulse pairs and for contiguous pulse pairs are used to explore the relative performances of the two velocity perturbation estimators, shear and spread.

The equations for the expected variance of the mean velocity estimates, the estimated bias of the velocity spread estimates and of the expected variance of the velocity spread estimates for both contiguous and independent pulse pairs (Zrnić, 1977) were used to compare the behavior of the Doppler spread and Doppler velocity estimators as a function of the signal-to-noise ratio*. Analysis was performed for a hypothetical S-band (10 cm wavelength) weather radar with a 1° beamwidth operating at a prf of 1000. For this radar system, the maximum observable Doppler velocity (Nyguist velocity) is ± 25 m/s and the maximum observable Doppler spread is 11.25 m/s.

The expected standard deviations of Doppler velocity estimates from estimators employing 64 independent or 64 contiguous pulse pairs are presented in Figure 2 for two different standard deviations (widths) of the true Doppler velocity spectrum, $\sigma_v = 1$ m/s and $\sigma_v = .2$ m/s. At σ_v equal to 1 m/s, the radar would take sample pairs spaced by 50 or more pulses to ensure independence, requiring a minimum of 3.3 seconds to

*Zrnić (1982) provided revised calculations including corrections to Zrnić (1977) and Doviak et al (1979).

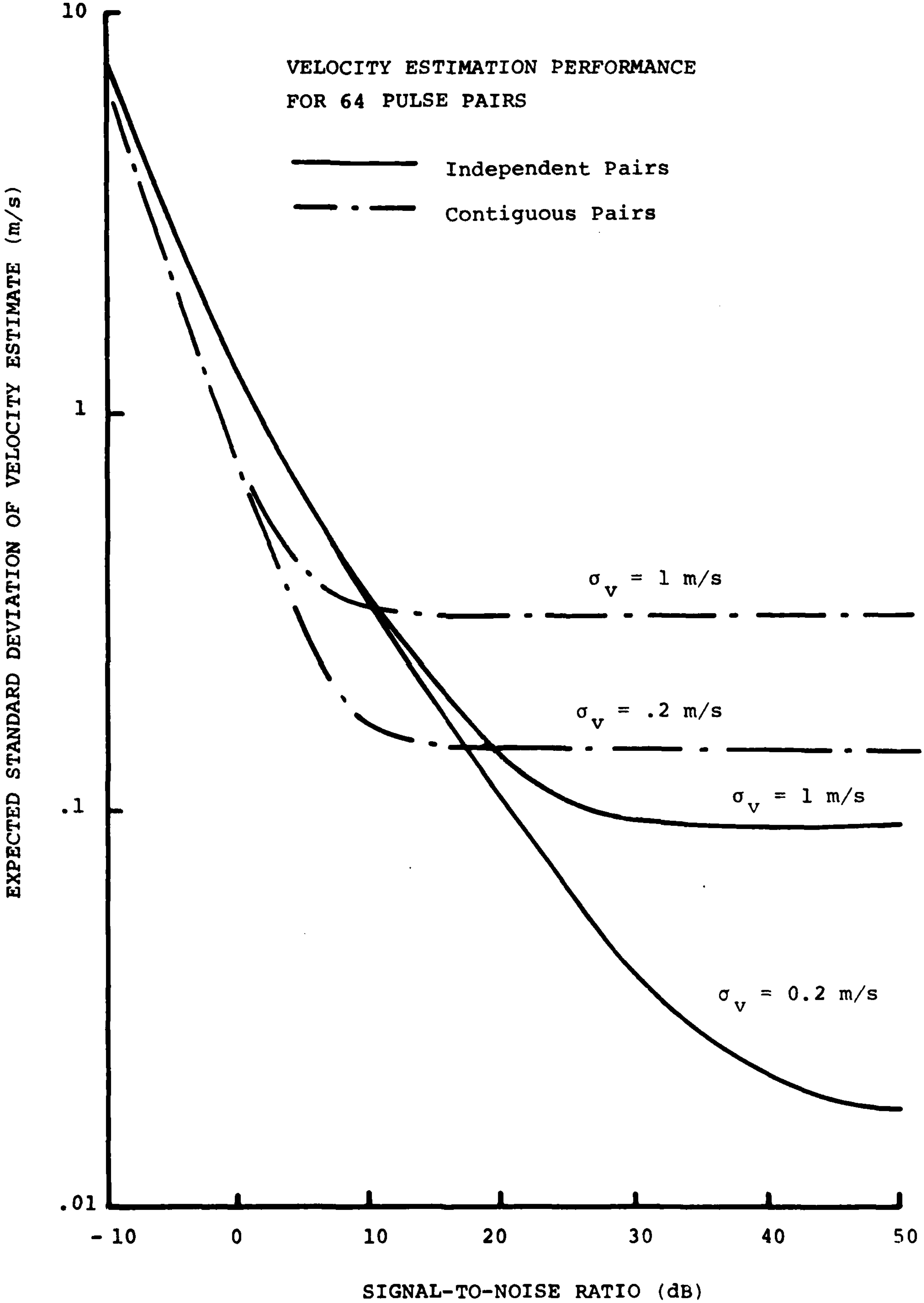

FIGURE 2. Performance of contiguous pulse pair and independent pulse pair estimators of the Doppler velocity.

acquire enough data for an estimate. At σ_v equal to 0.2 m/s, 16 seconds would be required to obtain a velocity estimate using independent pulse pairs. If contiguous pulses were employed, 65 pulses are required to form an estimate taking only 0.065 seconds. At one estimate per beamwidth, a complete azimuth scan would take 24 seconds using contiguous pulse pairs, 20 minutes for independent pulses if σ_v = 1 m/s and 1.6 hours if σ_v = .2 m/s. Practically,Doppler radars will use contiguous pulse pair estimators.

The difference between the two estimator types, independent and contiguous is evident at high signal-to-noise ratios in Figure 2. The improvement in the estimate (reduction in the standard deviation) is approximately half the square root of the time required to prepare an estimate. At low signal-to-noise ratios, this improvement is not realized and the contiguous pair estimator is superior. If, for example, a 1 m/s standard deviation in the estimate of Doppler velocity is tolerable, the contiguous pair estimator could be used when the signal-to-noise ratio exceeds -2 dB but the independent pulse pair estimator would require a +2 dB signal-to-noise ratio.

The expected value of the Doppler spread estimate is displayed in Figure 3 when 64 pulse pair values are used (independent or contiguous) to form the estimate and the true velocity spread is 1 m/s. Two estimates are displayed, one, using an asymptotically unbiased estimator employing signal-to

noise correction and, two, an older version of the estimator which does not employ signal-to-noise correction (Novick and Glover, 1975). The sign of the expected value changes at a signal-to-noise ratio near 8 dB but most estimators report only the magnitude of the value. For the asymptotically unbiased estimator, no bias exists for the example presented in Figure 3 for signal-to-noise ratios in excess of 20 dB. The departure from the true (1 m/s) value depends upon the number of sample pairs and, if the radar were to be operated with twice the number of sample pairs the departure would be half as large.

The expected standard deviation of the Doppler spread is presented in Figure 4. Again, the examples are given for 64 independent pulse pairs and 65 contiguous pulses (64 pairs) and a true velocity spread of 1 m/s. For these estimators, the differences are larger than for the Doppler velocity estimates. If an uncertainty in the spread estimate of 1 m/s could be tolerated, either estimator could be used provided a 10 dB signal-to-noise ratio is maintained for the data.

3.1.2 Relationship between Spread and Shear in a Turbulent Region - The velocity spread as observed by the radar may be caused by turbulence alone (no shear), shear alone (no turbulence) or a combination of shear and turbulence within the radar resolution volume. A number of other contributions to the uncertainty of the Doppler velocity or spread estimates are also

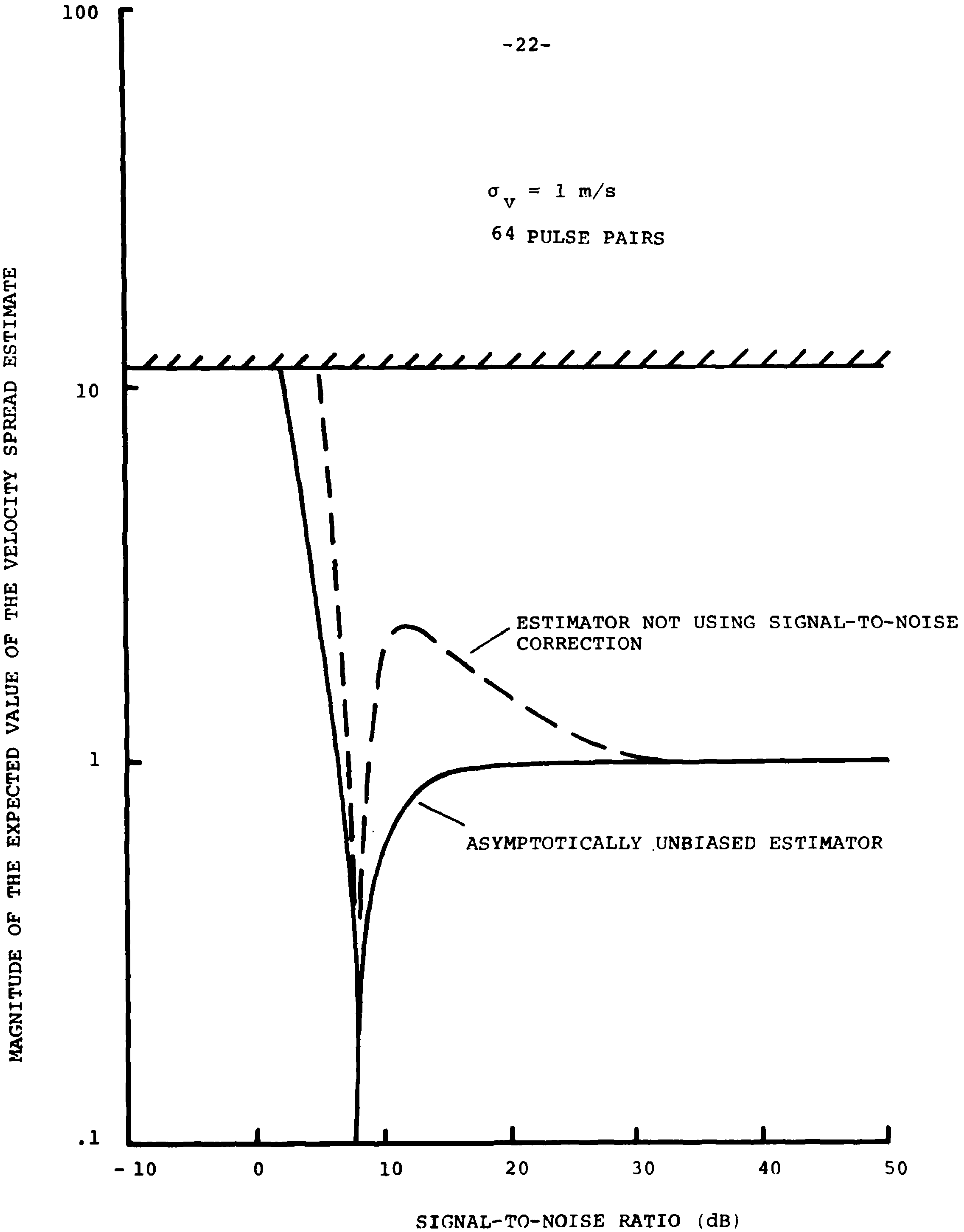

FIGURE 3. Doppler spread (spectrum width) estimation bias.

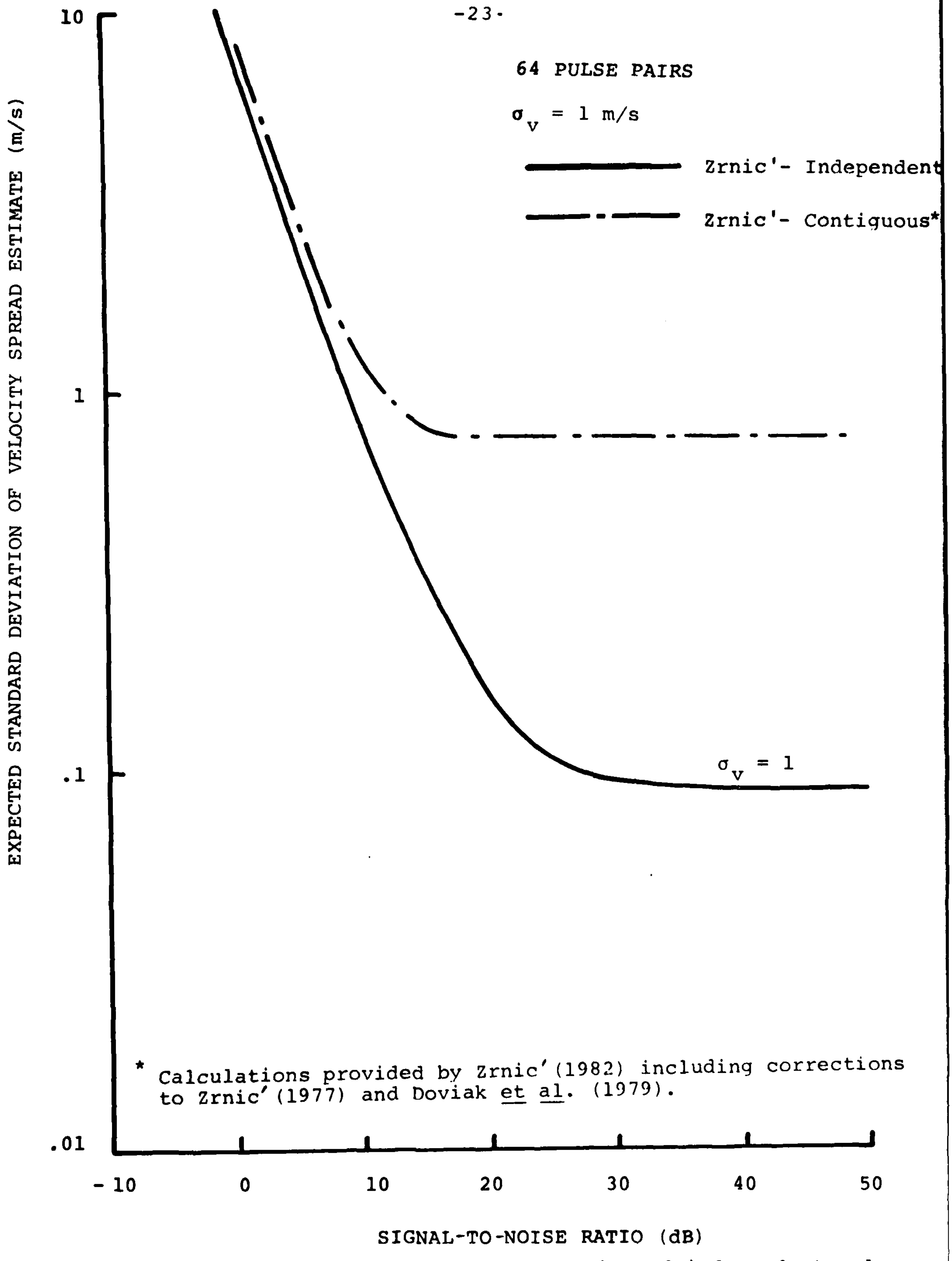

<u>FIGURE 4</u>. Performance of contiguous pulse pair and independent pulse pair estimators of the Doppler spread (spectrum width).

possible, interalia ground clutter contamination, aliased precipitation echoes, sidelobe contributions, variations in drop fall speeds when observing at higher elevation angles, and the variation of the radial velocity of a constant vector wind velocity due to the thickness of the radar beam (Doviak et al., 1979). The most important contributions are turbulence and shear. For a uniform shear and no turbulence, the Doppler velocity spread for a Gaussian shaped antenna directivity pattern is

$$\sigma_v = 0.3\ S(\frac{\pi R\theta}{180}) = 0.0052\ SR\theta \qquad (1)$$

where σ_v is the true velocity spread (m/s), S is shear (m/s/km), R is range (km) and θ is the half power beamwidth (one way - deg).

The separation of the velocity perturbation field into turbulence and shear contributions is somewhat arbitrary, both are always present in the convective flow field. Shear is often used to represent a linear approximation to the average change in velocity across more than one radar resolution volume, turbulence to represent everything else especially on a smaller spatial scale. The concept of isotropic, inertial sub-range turbulence applies only to the small scale fluctuations in the wind velocity about the larger scale variations sometimes described as shear. Isotropic turbulence, however, only occurs on scales smaller than the outer scale which, for convective

larger than observed by the aircraft. They concluded that a small scale region of large shear, shear on a scale smaller than the radar system cross-beam resolution (50 km range, 1° beamwidth), was responsible for the extreme spread observation. As with other aircraft-radar comparisons, the region was turbulent but the spread observations could not be used as a measure of the intensity of the turbulence. A large shear existed in the same region but it also could not be used to estimate the intensity of the turbulence.

3.1.3 Relative Merits of Spread and Shear Estimates - The relative merits of shear or spread estimates for the detection of velocity perturbation can be assayed only when a relationship is assumed between the true shear and true spread to be observed by the radar. High resolution Doppler spectrum observations of turbulence in the clear atmosphere show that shear and spread always coexist and, in small subregions of the radar resolution volume, the spread is often the order of 0.2 m/s although the spread in the signal from the entire resolution volume can exceed 1 m/s (Crane, 1980).

Morphological studies of the spread of the Doppler spectrum for quiet regions of widespread rain surrounding severe storms indicate that the spread is typically between 1 and 2 m/s (JDOP, 1979, Figure 6 at 80 percent or higher) and that the median value is about 4 m/sec. Waldteufel (1976) reported storm average values of the vertical shear of the

turbulence is often smaller than the cross-beam resolution ($\pi R\theta/180$) of the radar system (Crane, 1981; Bohne, 1981).

The eddy dissipation rate of the isotropic, inertial subrange turbulence is the parameter usually associated with aircraft turbulence and is estimated from onboard instrumentation during aircraft penetration flights. No known relationship exists between larger scale gradients of the average velocity fields and the smaller scale eddy dissipation rate other than the observation that the power spectral density of the velocity fluctuations generally decrease with decreasing scale size. If the outer scale for isotropic, inertial subrange turbulence is larger than the maximum radar resolution volume and no shear of the average wind is present (a rare occurrence) the Doppler spread measurements can be interpreted as measurements of the eddy dissipation rate. Otherwise, the Doppler spread measurements must be interpreted as velocity perturbations (shear) on the scale of the radar resolution volume and shear measurements (the average difference in velocities between two resolution volumes divided by the resolution volume separation) must be regarded as observations of velocity perturbations (shear) on a slightly larger spatial scale.

Hjelmfelt et al. (1981) observed a small region of extreme velocity spread and nearly simultaneously probed the region with the SDSMT T-28 aircraft. They found that the extreme spread implied an eddy dissipation role more than an order of magnitude

horizontal wind as varying from 2 to 6 m/s/km depending on height and of the horizontal shear of the horizontal wind as averaging about 4 m/s/km independent of height. He also reported a weak correlation between the horizontal shear of the horizontal wind and the velocity spread (after correction for shear).

Noting that for both studies, the average radar range to the spread or shear observations was of the order of 60 km, and, at a range of 60 km, a shear of 4 m/s/km equates to a Doppler spread of 1 m/s for a 0.8 degree beamwidth system (NSSL radar parameter), a reasonable model for the widespread precipitation region surrounding a storm is that a 3.2 m/s/km shear (S) produces a 1 m/s spread (σ_v) for a 1 degree radar beamwidth at a range of 60 km. This S, σ_v pair corresponds to values below the reported mean values, better representing the quiet, non-hazardous regions of a storm. The weak correlation between shear and spread after correction for shear noted by Waldteufel is consistent with this model and the understanding that a linear shear is only an approximation to the more complex, variation in wind velocity on the scale of several cross-beam resolution distances (≃ 2 km).

With the simplified relationship between spread and shear, the merits of each velocity perturbation estimator can be assayed relative to the false alarm problem. From the Kansas observations Crane and Hardy (1981) found that, on average,

15 percent of the radar surveillance area was covered by echo. Assuming a 0.25 km by 1 deg. resolution volume, 2 false detections (alarms) per scan correspond to a 3.95 standard deviation departure from the expected value of the Doppler spread or difference between the velocity estimates between two adjacent resolution volumes (shear). The uncertainties in velocity estimation are assumed to be independent between adjacent resolution volumes. The results of using these assumptions for observations at a range of 60 km are displayed in Figure 5 for an independent pulse pair estimator and in Figure 6 for a contiguous pulse pair estimator when the shear contributing to the observed spread is vertical. In each case the asymptotically unbiased, spread estimator (solid curve, Figure 3) was assumed.

Calculations are displayed for 3 different false alarm rates (2, 20, or 200 per scan) in Figure 5 and the two extremes (2 and 200 per scan) in Figure 6. Three scales are presented, velocity spread estimate, velocity difference estimate (between 2 adjacent resolution volumes) and tangential shear estimate. These are related by equation (1). The tangential shear, S, equals the velocity difference divided by the cross-beam resolution distance. The relatively close spacings between the curves for different false alarm rates (FA) for the same estimators indicate that only a small change in signal-to-noise ratio is required to go from essentially no false alarms to a

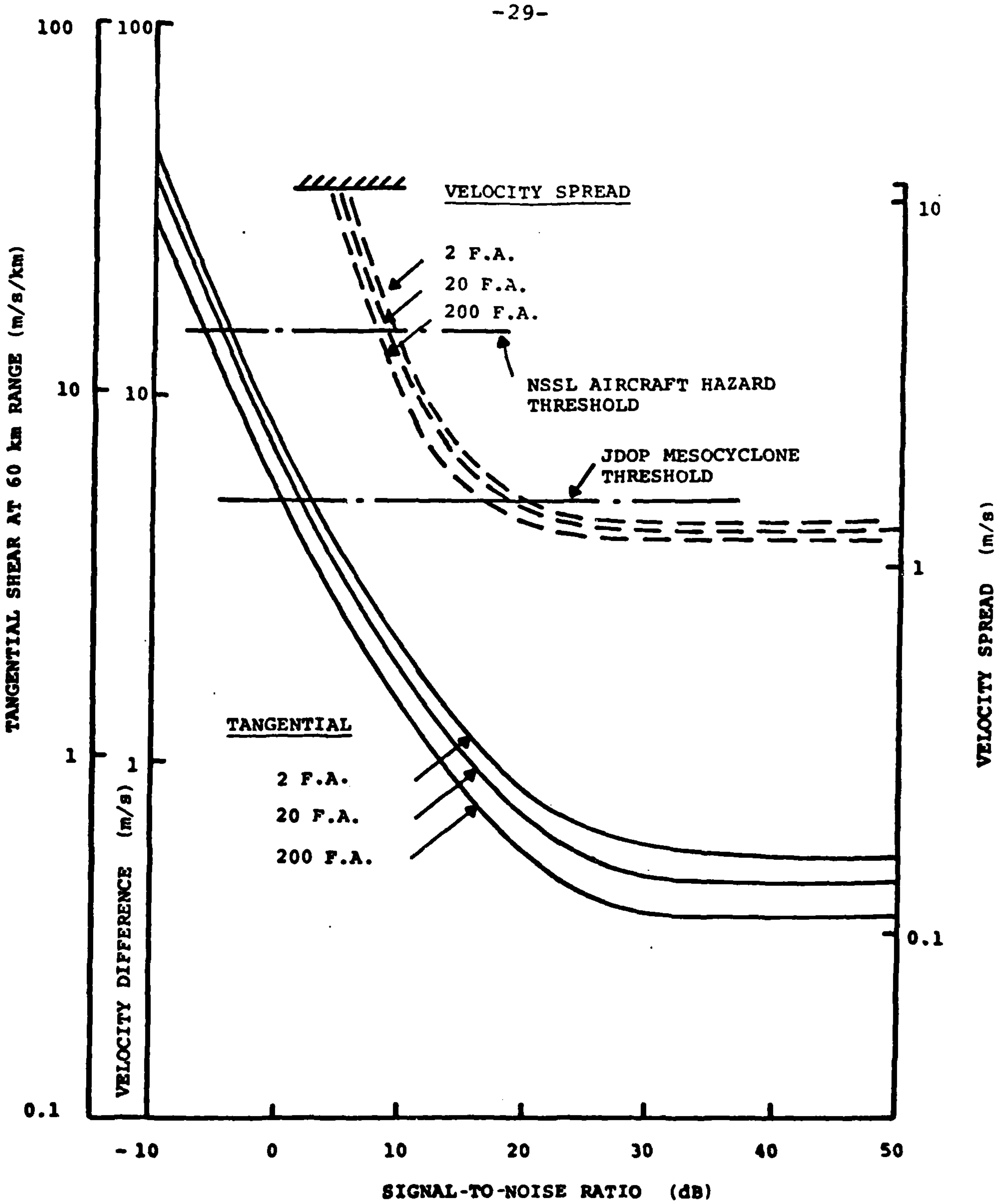

FIGURE 5. Relative performance of Doppler spread (spectrum width) and tangential shear estimators when the true spectrum width is produced by a vertical shear of 3.2 m/s/km. Results for 64 independent pulse pairs.

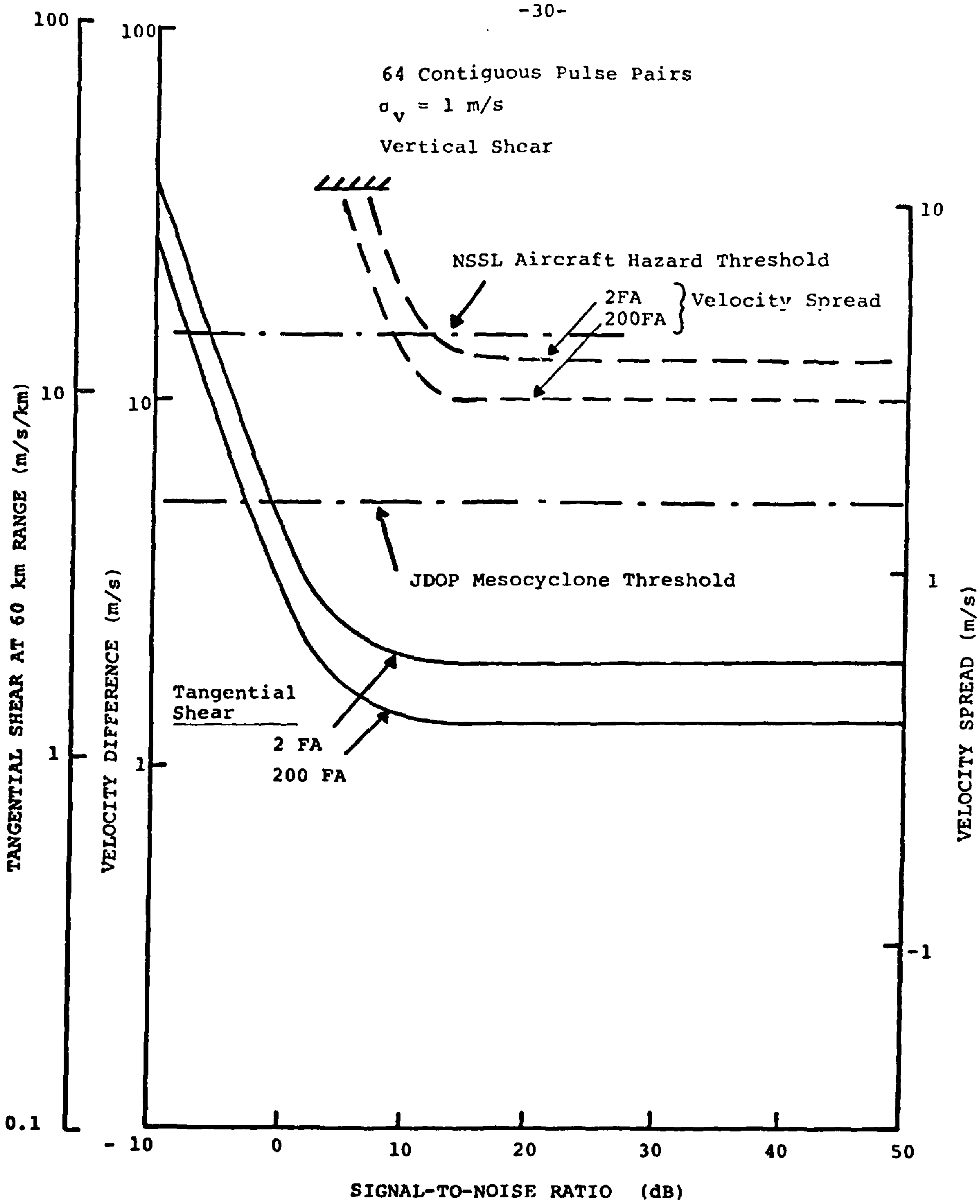

FIGURE 6. Relative performance of Doppler spread (spectrum width) and tangential shear estimators when the true spectrum width is produced by a vertical shear of 3.2 m/s/km. Results for 64 contiguous pulse pairs.

situation with an extreme number of false alarms. This behavior was noted in the NHRE data and prompted the use of signal-to-noise dependent thresholds for further processing.

Two hazard detection thresholds are displayed on the figure, the mesocyclone detection threshold proposed by JDOP (1979) and the aircraft hazard detection threshold proposed by Lee (1977). As derived, only shear data should be used for mesocyclone detection but, as discussed above, either shear or spread could be used for aircraft hazard detection. Clearly, for the conditions of Figures 5 and 6, the use of spread estimates produces a higher false alarm rate at a given signal-to-noise ratio. Using contiguous pulse pairs, a minimum 15 dB signal-to-noise ratio is required if spread is to be used but only a zero dB signal-to-noise ratio is required if shear is employed (0 dB to allow successful mesocyclone detection as well).

The assumed 1 m/s velocity spread could also be produced by horizontal shear. This case is depicted in Figure 7 for the contiguous pulse pair estimator. For this example, the observed shear is assumed to be the expected, 3.2 m/s/km background shear plus the statistically variable component corresponding to the indicated number of false alarms per scan. For aircraft hazard detection, the signal-to-noise values at the detection threshold differ by at most 3 dB from the values for the same FA in Figure 6 but, for mesocyclone detection, a 3.2 m/s/km background shear is sufficiently close to the 5 m/s/km

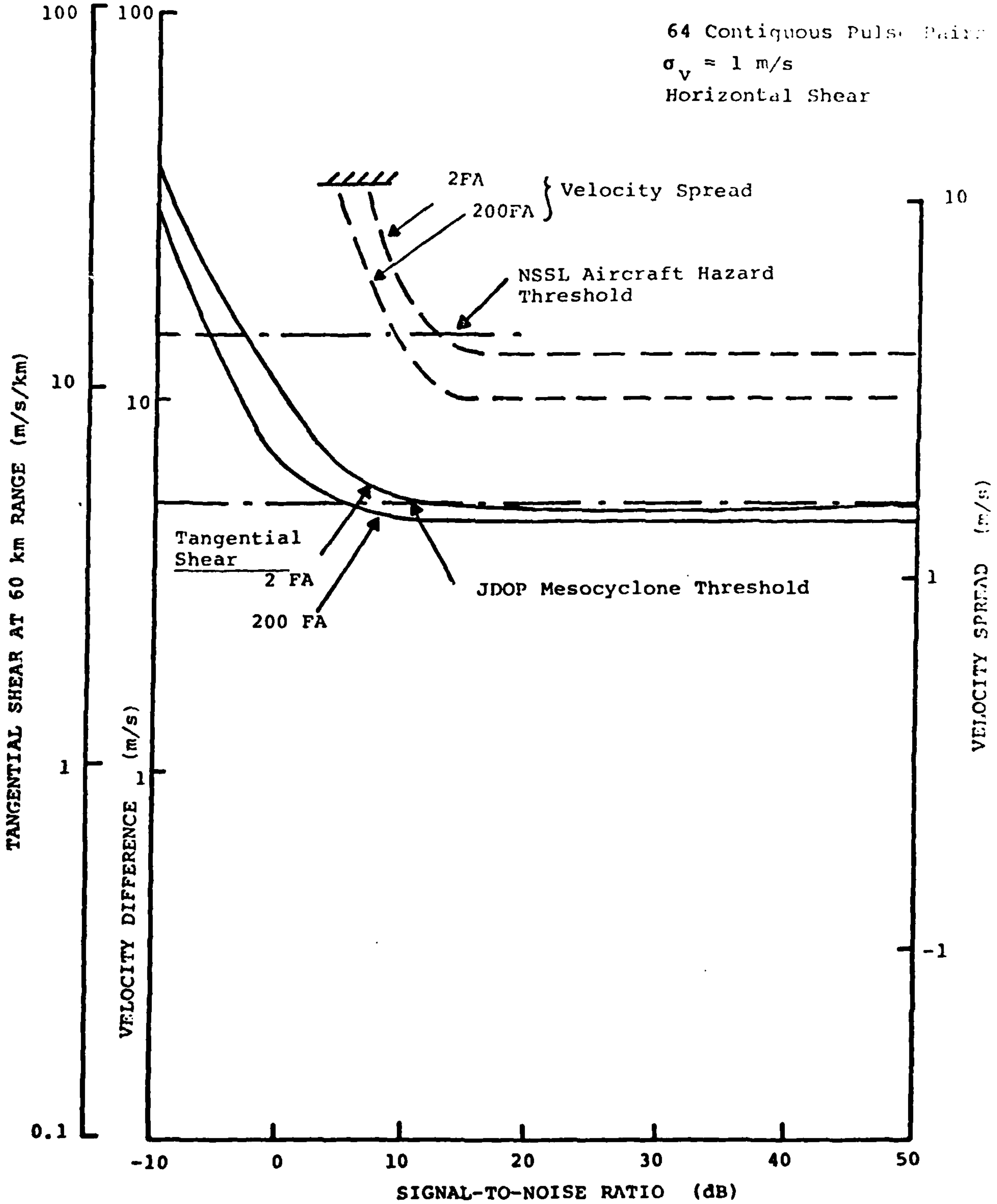

FIGURE 7. Relative performance of Doppler spread (spectrum width) and tangential shear estimators when the true spectrum width is produced by a horizontal shear of 3.2 m/s/km. Results for 64 contiguous pulse pairs.

threshold to cause 2 or more FA per scan at any signal-to-noise ratio. To consistently separate the 3.2 m/s/km, background value from the 5 m/s/km mesocyclone, more filtering is required.

In summary, at the same shear or equivalent spread values, the shear estimator is superior to the spread estimator in terms of signal-to-noise behavior. Over the range of values dominated by the noise statistics (the steeper regions of the curves) the shear estimator has at least a 15 dB advantage over the spread estimator. The comparison was made for a range of 50 km. At shorter ranges the performance of the spread estimator improves relative to the shear estimator (see Eq. 1) but at longer range the opposite is true. Equivalent behavior is not obtained at any range due to the steepness of the spread estimation curves at low signal-to-noise ratios.

3.2 Requirement for Spatial Filtering

The statistical properties of the shear and spread estimators imply that measurements may be made with a low false alarm rate only when the signal-to-noise ratio exceeds some threshold. If measurements are to be attempted at lower signal levels, additional averaging or filtering is required. Since observations are desired in the weaker echo regions during the initial phases of convective cell development, filtering will always be required.

The hypothetical radar model used to calculate the behavior

of the velocity and spread estimators was based on an assumption of 64 pulse pairs requiring 65 pulses (contiguous pairs). For the assumed parameters, a single azimuth scan would take 24 seconds and a complete tilt sequence at 18 elevation angles would take over 7 minutes. In practice, radars are designed to use fewer than 64 pulse pairs to keep the time for a tilt sequence down to about 5 minutes. With fewer pulses, the statistical uncertainties increase relative to the values displayed in Figure 2 through 7.

The NCAR and NOAA Wave Propagation Laboratory (WPL) Doppler radars used to collect data for the NHRE case studies employed either 32 or 64 contiguous pulse pairs for the estimation of velocity. Experience with these radars indicated that at the 1 m/s/km threshold used for shear cell processing, a large number of false cells were detected. Reference to Figures 6 and 7 indicates that a number of false alarms were to be expected at all signal-to-noise ratios. Due to the expected (and observed) anisotropy of the shear field, the lowest possible processing threshold is desired since the maximum shear value in a perturbed region cannot be observed with a single radar. The successful use of a low shear processing threshold was demonstrated by Crane (1981) for hazard detection but the problem of reducing the number of false alarms remains.

One step in the filtering process used to reduce false

alarms is to require continuity of a region of shear in height and time. This continuity requirement was built into the JDOP mesocyclone detection algorithm (JDOP, 1979) by requiring that a region of shear persist for a half period of a vortex revolution (5 to 15 minutes) and extend vertically through a height interval comparable with the horizontal diameter (minimum of 3 elevation angles). It was also used in the cell tracking algorithms by requiring cell continuity (tracking) between volume scans and more than 3 shear cell detections in a volume scan (Crane, 1981).

Experience with the use of continuity for filtering the NHRE case study data showed that the false volume cell detection problem was reduced significantly as long as the initial false alarm rate was small but when the initial false alarm rate was high, continuity could be established by chance. In effect continuity on successive scans (in elevation and between tilt sequences) is equivalent to increasing the number of samples processed to make a detection. Since a minimum of 6 samples were combined as a part of the continuity test, a factor of 2.5 reduction in the standard deviation of the estimate (Figures 2 and 4) and a factor of 6 reduction in the bias component (Figure 3) could be obtained. Referring to Figure 7, the result is to move the 2 FA curve for tangential shear down to 4 m/s/km from above the 5 m/s/km threshold at signal-to-noise ratios in excess of 10 dB.

Finally, to provide additional independent samples to further reduce the standard deviation of the shear (or spread) estimates, spatial filtering is required. Spatial filtering can be easily achieved in range by smoothing the velocity fields in range prior to calculating the value of the shear. Additional smoothing in azimuth can be achieved if recursive filters are used or data are stored in the computer at a number of azimuth positions to allow fixed weight moving average filtering. Data preparation for multiple Doppler radar analysis usually requires preprocessing with spatial filters with a 2 to 3 km radius of influence. The requirement to increase the number of samples for each velocity estimate (smoothed) suggests that moving average filters equivalent to a uniformly weighted average over 3 successive range and 3 successive azimuth intervals be employed resulting in a factor of 3 reduction in the standard deviations.

The spatial filter will suppress the high spatial frequency noise components but still pass information useful for the calculation of shear on the scales required for mesocyclone detection and for the location of in flight aircraft hazard. If, following McCarthy et al., (1976), it is assumed that velocity variations on the scale of the aircraft phugoid frequency at the normal aircraft speed during landing and takeoff are of importance for the detection of hazardous wind shear close to an airport,

then for jet aircraft similar to a Boeing 727, spatial averaging is possible as long as fluctuations on spatial scales the order of 1 km are passed through the filter with little attenuation. Since terminal area observations will be made at short ranges, azimuthal or temporal averaging may be more acceptable than range averaging for increasing the effective number of samples.

3.3 Additional Attributes for the Detection of Hazard

The false alarm problem has two origins, one caused by the statistical uncertainty in the estimation of a value of shear (or spread) considered in sections 3.1 and 3.2 and, two, caused by uncertainty in the existence of a region of hazard given an exact measurement of the shear (or spread). The latter problem occurs for either shear or spread measurements because, for a radar resolution cell with a maximum dimension of more than 400 m (distances greater than 28 km for a 1° beam radar averaged and sampled every 1°), velocity fluctuations on scales larger than the outer scale for the inertial subrange component will dominate the observations. These larger scale fluctuations are aspect sensitive (depend on the relative locations of the radar and perturbation regions) and cannot be used to uniquely determine the existence of a region of hazard. If, for landing or takeoff, the velocity fluctuations on scales which will excite the phugoid frequency resonance of an aircraft are also to be observed (McCarthy et al., 1979), direct measurement is again not possible unless the radar is located on the airport

because of the vertical variation and anisotropy of the velocity fluctuations. In either case, the existence of a possible aircraft hazard can only be inferred, not directly observed.

Analyses of aircraft penetration flight data have shown poor correlations between the magnitude of the hazard (intensity of the turbulence) and the magnitude of the shear or spread. Since the hazard detection problem is one of inference and not direct measurement, some uncertainty is to be expected. The uncertainty can perhaps be reduced by incorporating additional data in the hazard detection algorithm. Crane (1981) noted that the intensity of the turbulence in the near vicinity of a convective cell depended on the age of a cell. He also noted that cells which showed little change in horizontal momentum with height within the updraft region were more likely to be associated with the more extreme turbulence levels. These observations suggest the use of volume cell or cluster age and the vertical variation in radial velocity within a cell or cluster of cells as additional attributes for hazard detection.

Other additional attributes may also be useful. The location of the cell or cluster relative to the overall pattern of cell development may be important. The mode of initial development or growth may also be important. Observations in Kansas (Crane and Hardy, 1981) and in

Colorado (Crane, 1981) have shown that cells with reflectivities above 40 to 45 dB that form high in a cluster (at heights above 7 km) are indicative of hail formation. Cells with reflectivity maxima that ascend during growth may also be indicative of active regions of convection while cells which form at the height of the melting level then settle to the ground are indicative of the random clumping of debris away from the regions of active growth. Each of these attributes provide additional data useful for inferring the existence of hazard.

The attributes identified in this section, age, vertical variation in radial velocity, initial ascent or decent of the reflectivity weighted average cell height, initial cell height for cells in clusters, and cell location relative to prior cell development have been incorporated in the detection and tracking algorithms as indicative of a significance level or class for the cell. The use of the attributes have not been tested due to a lack of adequate, continuous Doppler radar observations and simultaneous aircraft penetration flights.

4. ALGORITHM REFINEMENT

The cell detection and tracking algorithms were refined to (1) provide signal-to-noise level thresholds for subsequent processing, (2) include spatial filtering for the preparation of velocity and shear estimates, (3) revise the tracking algorithms to accommodate the widely spaced elevation angles of the NSSL data set, to associate more than one velocity perturbation cell with a volume cell, and to provide a multilevel significance estimate for hazard detection, (4) prepare concatenated vector output from the contouring algorithm for graphical display, and (5) to prepare the graphical displays. A detailed description of the program revisions are included in Gustafson and Crane (1981).

The computer programs resident on the Department of Interior, Cyber 74 computer that were used for the analysis of the NHRE case study data (Crane, 1981) were transferred to the FAA supported DEC VAX 11/780 computer operated by the MITRE Corporation in McLean, Virginia. Program preparation and data processing were accomplished via telephone from the ERT offices in Concord, Massachusetts.

4.1 Preprocessing

The computer programs installed on the VAX 11/780 were revised to accept Doppler radar data from the Norman

and Cimarron radars of the National Severe Storms Laboratory (NSSL). The revised programs accept the NSSL data tapes, perform the required calibration operations, and supply the data for use by the cell detection and tracking program.

The preprocessing program automatically resolves the range ambiguity of the Doppler data using the reflectivity data from the dual prf system in use at NSSL. The velocity unfolding algorithm previously used for the NCAR data was revised to accept the NSSL data and to incorporate thresholding and spatial filtering. The signal-to-noise ratio for each (range unfolded) Doppler return is estimated from the receiver noise level reported by NSSL and the reflectivity value from the reflectivity data. The signal-to-noise ratio is required to be above 10 dB to further process the velocity estimates and above 15 dB to further process Doppler spread estimates.

After thresholding, the data are unfolded in velocity by minimizing first the velocity difference between adjacent range gates by calculating the Nyquist interval to minimize the difference, second by minimizing differences relative to the Nyquist interval between the observed velocity and the smoothed velocity data for the same range gate from the prior azimuth position and finally by minimizing the difference between the velocity estimate and a moving average (in range) velocity estimate for the same range interval.

After unfolding, the data are smoothed by a weighted

recessive filter in azimuth. The weights were set to make the averaging region roughly circular with a 3 km radius at a 60 km range. The smoothed data were used to calculate range, tangential and total (square root of the sum of the square of the range and tangential) shear.

4.2 Tracking

The cell detection program is separately operated on the reflectivity data field and on one of the velocity perturbation fields. The velocity perturbation field, spread or shear, to be used is selectable at the time the program is run.

The tracking program was modified to associate one or more velocity perturbation cells with a volume cell. The program operates using first the reflectivity cells and second the velocity perturbation cells. If no volume (previously declared) cell is close enough to a velocity perturbation for association, the velocity cell is used to create a new volume cell. In this way, all the velocity perturbation regions are taken into account but if more than one region of shear (or spread) is associated with a volume cell, multiple volume cells are not generated.

The tracking program was also modified to calculate only the reflectivity weighted average height of the volume cell instead of the peak, and heights on the reflectivity profile for the cell 3 dB below the peak. A statistical

analysis of the height information in the Kansas data set showed that the 4 measures of height, peak, reflectivity weighted average and the two 3dB-down-from-peak heights were highly correlated and only one was required to characterize the profile.

Cell age was added to the list of cell attributes and the relative heights of the cell on the first two volume scans for the cell are used to calculate a cell attribute. The average radial velocity and root mean square (rms) spread of the radial velocity for all observations, reflectivity, and velocity perturbation are calculated as cell attributes. Under normal program operation, both the average tangential shear and Doppler spread for the volume cell are calculated as attributes. The latter pair could change depending upon the estimator of velocity perturbation used for cell detection. The numbers of reflectivity cells and velocity perturbation cells associated with a volume scan are also employed as volume cell attributes.

The initial data set received from NSSL were for tilt scans sequences having 3 deg. or more elevation steps between azimuth sector scans. The tracking algorithms developed for use with the Kansas and NHRE data sets were optimized for smaller elevation steps. The weights used to separate cirrus cloud detections from shallow cells in the debris region had to be modified to allow cell association across the large height gap at longer ranges.

4.3 Graphical Display

Graphical displays were generated to present the contour, cell and cluster data from the detection and tracking program. An example of the graphical display is given in Figure 1. The 20 dBZ contours and sector scan boundaries are shown as solid curves. The cell and cluster centroids are marked as + or x. Summary information for the volume scan were also tabulated on the side of the display. The dashed lines are 1.4 hour extrapolations along the smoothed tracking vectors for each of the clusters with an age of 3 or more volume scans. The extrapolation interval and minimum age are selectable interactively and the values in use for the display are indicated in the tabulated data.

The information to be displayed can be selected interactively. Both or either of two reflectivity contours can be displayed, the contour used for cell detection and a second contour level for display. For Figure 1 only the cell detection contour was displayed. A second contour level (typically 40 dBZ) could also be displayed.

The information generated for display, the cell, cluster and contour attribute lists and the concatenated vector contour lines are also recorded on magnetic tape for analysis or display at other facilities.

5. ANALYSIS OF NATIONAL SEVERE STORMS LABORATORY (NSSL) DATA

Two data sets were provided by NSSL for program development and data analysis. The first data set included both Norman and Cimarron radar observations for the 1015 to 1045 CST time period, June 17, 1979. This data set was used for program development (see Figure 1) and to intercompare data from the two radars. The second set included data from the Norman radar only for 0813 to 0953 CST, June 16, 1980. The later data set was used to test the tracking routines. No penetration data were available for either data set and, therefore, no further evaluation of the hazard detection algorithms was possible.

5.1 Intercomparison of Cimarron and Norman Radar Cell Detection Data

The 1979 data set was processed to provide volume cell data for the comparison of simultaneous observations of the same volume cells by the two radars. The intercomparison test was made to explore the aspect sensitivity of the velocity perturbation measurements. The NCAR C-band radars and NOAA WPL radars were intercompared as a part of the prior analysis of the NHRE case study data. In that comparison, the aspect sensitivity of the tangential shear measurements were evident. The comparison did show that the small reflectivity cells could be readily detected by several radars and

the reflectivity data could be intercompared to obtain the relative calibrations of the radars.

The results of the intercomparison study for the Norman and Cimarron radars are presented in Figures 8-10. Figure 8 displays simultaneous measurements of the average reflectivities of isolated volume cells from a single volume scan. Data were taken from the sector volume scan pair from the NSSL data set that was most nearly coincident in time and space. The median difference between the reflectivity values was 10 dB suggesting a 10 dB calibration difference between the two radars. This difference was subsequently confirmed by NSSL site personnel. The variation about the median line is 3.6 dB (rms), nearly the same as the 4.6 dB rms differences observed in the larger data set from the NHRE case study data.

The intercomparison between tangential shear values for the same isolated volume cells is depicted in Figure 9. As before, a fair variation about the equal value line is evident, a result indicative of anisotropy in the shear field. Isolated volume cells were chosen for analysis to ensure complete observation of the velocity perturbations associated with a cell without question about possible association with another volume cell. The volume cells were also chosen to have nearly identical vertical extents as observed by the two radars. The later requirement was set to ensure the

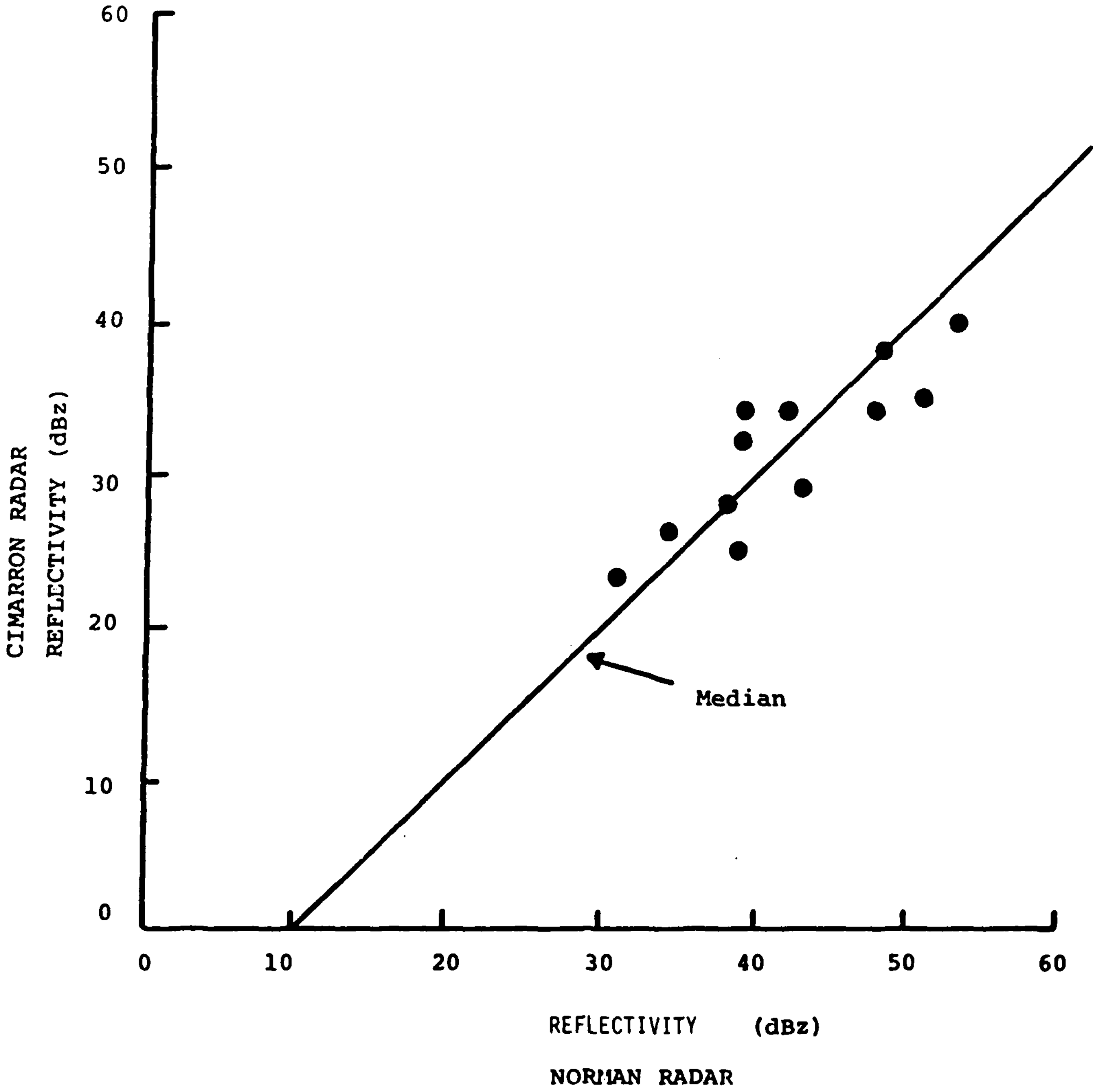

FIGURE 8. Intercomparison between simultaneous reflectivity measurements using isolated volume cells.

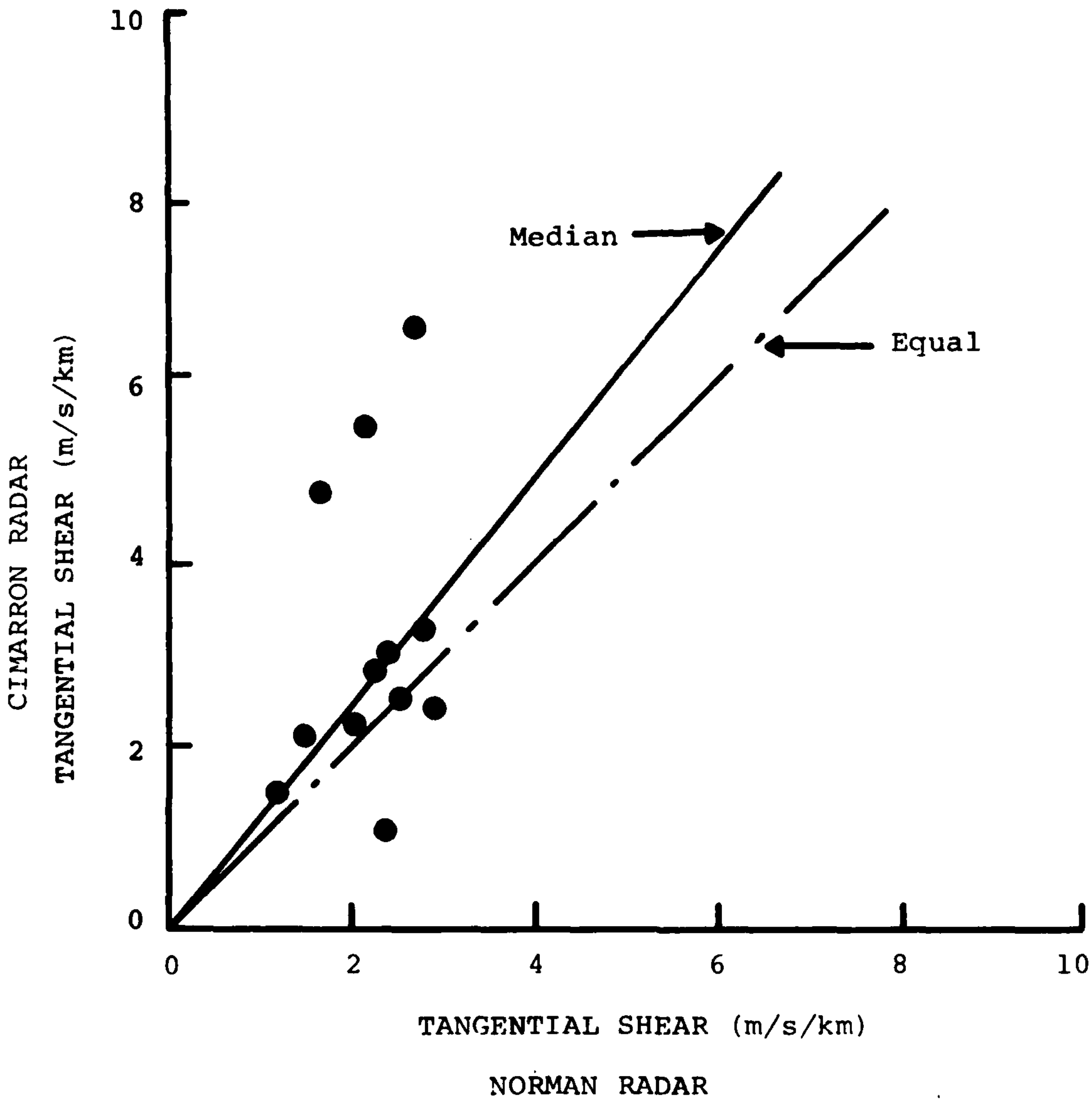

FIGURE 9. Intercomparison between simultaneous tangential shear measurements using isolated volume cells.

equivalence of the reflectivity and velocity perturbation fields for comparison.

The comparison between Doppler spread (spectral width) values is presented in Figure 10. The program was rerun using Doppler spread as the measure of velocity perturbation for cell detection to provide the data for this figure. As for tangential shear, a variation of spread values about the equal value line is evident. This result is again indicative of anisotropy or an aspect sensitivity of the velocity perturbation observations. Employing the 4 m/s threshold for aircraft hazard detection proposed by NSSL, only one third of the cells would have been classified as hazardous using the Norman data but three quarters of the cells would have been identified as hazardous using the Cimarron data. Unfortunately, due to a lack of penetration data, no information is available to ascertain how many of the cells were indeed hazardous.

Doppler spread and tangential shear are not the only possible measures of velocity perturbations. Wilson et al., (1980) advocate the use of radial shear instead of tangential shear. Radial shear is important for sensing the along-the-glide-slope variation in the longitudinal velocity of wind relative to an aircraft during landing or takeoff required for the detection of wind shear hazard (McCarthy et al., 1979) by a radar installed at the airport. For surveillance using a weather radar not installed at an airport or for

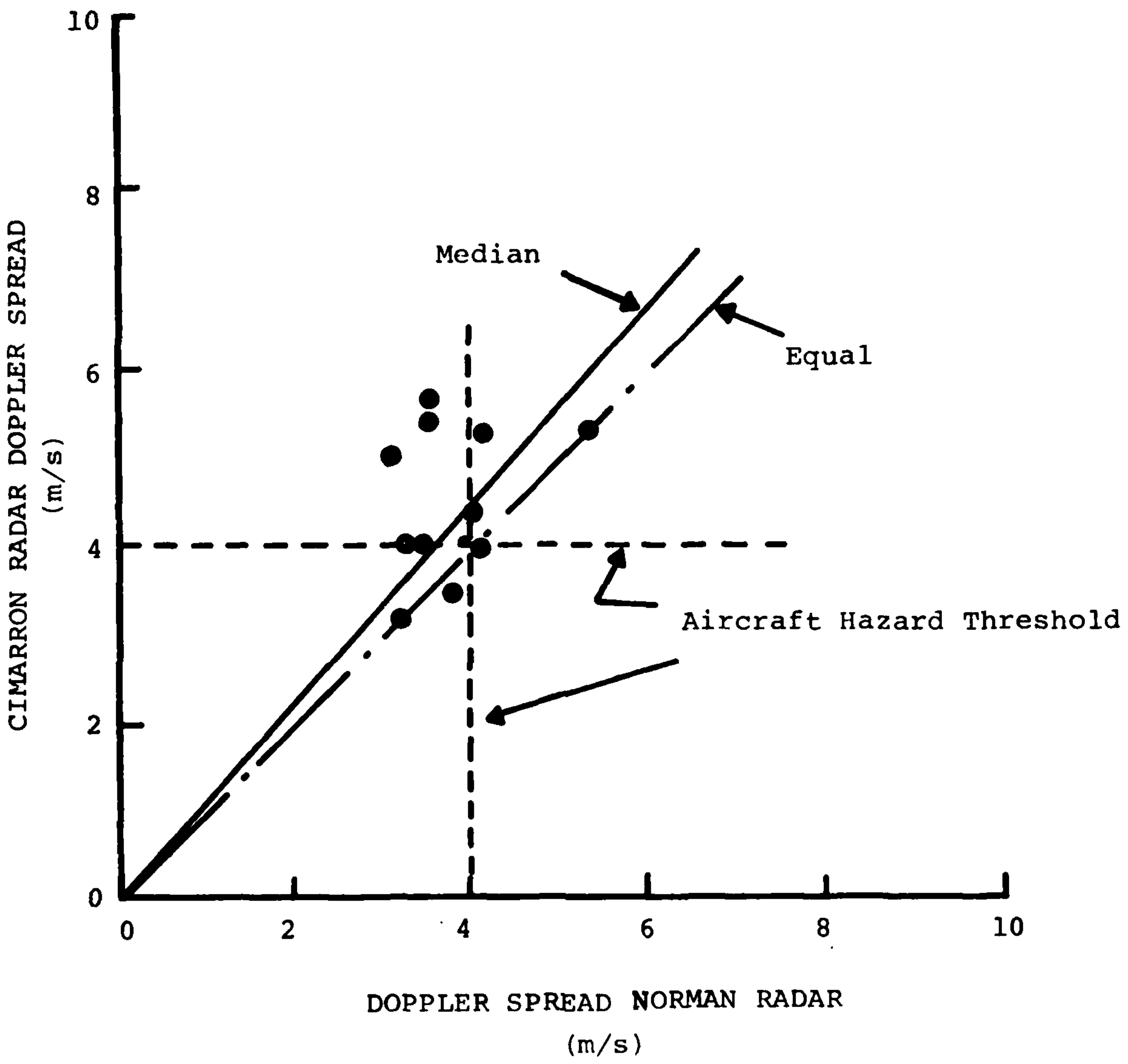

FIGURE 10. Intercomparison between simultaneous Doppler spread (spectral width) measurements using isolated volume cells.

the detection of severe weather over a wider area, tangential shear may be a better choice than radial shear.

The cell detection program was rerun on the NSSL data using radial shear as the measure of velocity perturbation. The results are displayed in Figure 11. Only 9 of the 12 isolated volume cells were detected by the Cimarron radar while 10 of the cells were detected by the Norman radar. In contrast to the use of Doppler spread or tangential shear, radial shear observations did not provide as high a volume cell detection probability (based on this limited data set). For the cells that were detected using both the radial shear measure of perturbation and the tangential shear measure, most of the observations were tightly clustered about the median line suggesting a high degree of correlation between tangential and radial shear (for those volume cells). The outliers, away from the median curve, may be in response to the variation in anisotropy of the wind field across the surveillance region common to both radars. A much larger data set must be processed to decide if the radial shear data is redundant or provides additional information useful for reducing the false hazard detection (false alarm) problem

5.2 Tracking Analysis

The 1980 data set contained a 1.7 hr continuous set of sector volume scans useful for evaluating the refinements in the cell association and tracking algorithms. Summary water

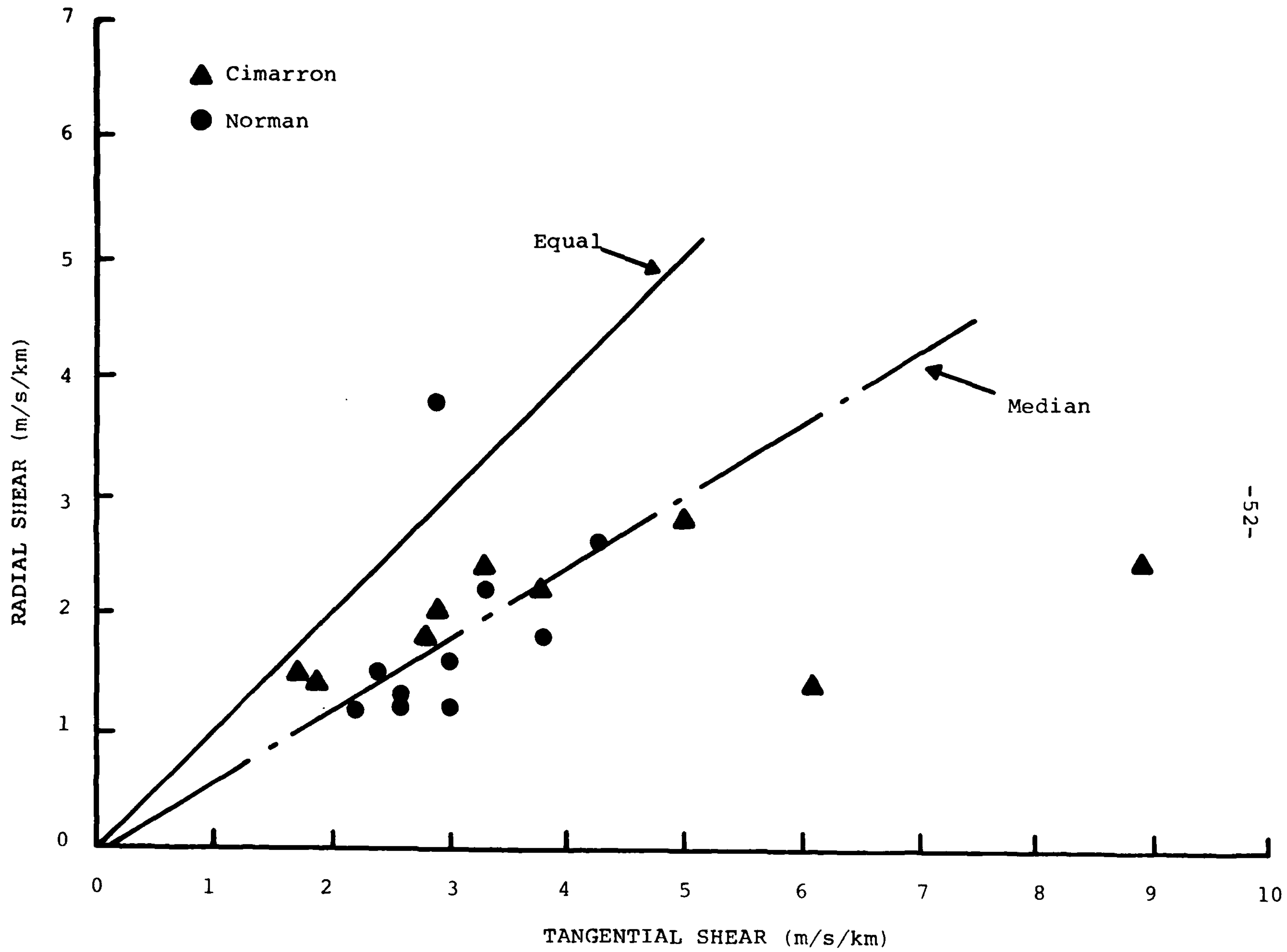

FIGURE 11. Intercomparison between tangential shear and radial shear measures of velocity perturbation for the same isolated volume cells.

flux and echo area data are depicted in Figure 12 for the azimuth sector scan at the lowest elevation angle. A decrease in water flux was evident throughout the 0813 to 0929 time period accompanied by a more gradual decrease in echo area. The active region of the storm was moving through the radar surveillance area. Adjustments in the sector boundaries were then made to provide surveillance over the more active regions of the storm. The adjustments in sector boundaries were also evident in the numbers of volume cells and numbers of significant cells and clusters tracked during the observation interval (Figure 13) and in the average track velocity transients (Figure 14).

A number of tracking results are displayed in Figures 13 and 14 to describe the behavior of the tracking algorithms under different operating conditions. The tracking program was run using (1) all the reflectivity and tangential shear data, (2) reflectivity data only, (3) tangential shear only, and (4) reflectivity plus tangential shear data but with a restart of the tracking operation if the predicted cell location was more than 3.0 km from the observed cell location.

Tracking runs (1) and (4) used the same cell detection data but different data for initializing the velocity for each track. Track initialization employed the average, smoothed track velocity data (depicted in Figure 14) from the prior volume scan. The tracking run with the track velocities reset to the smoothed track velocity (run 4) produced the

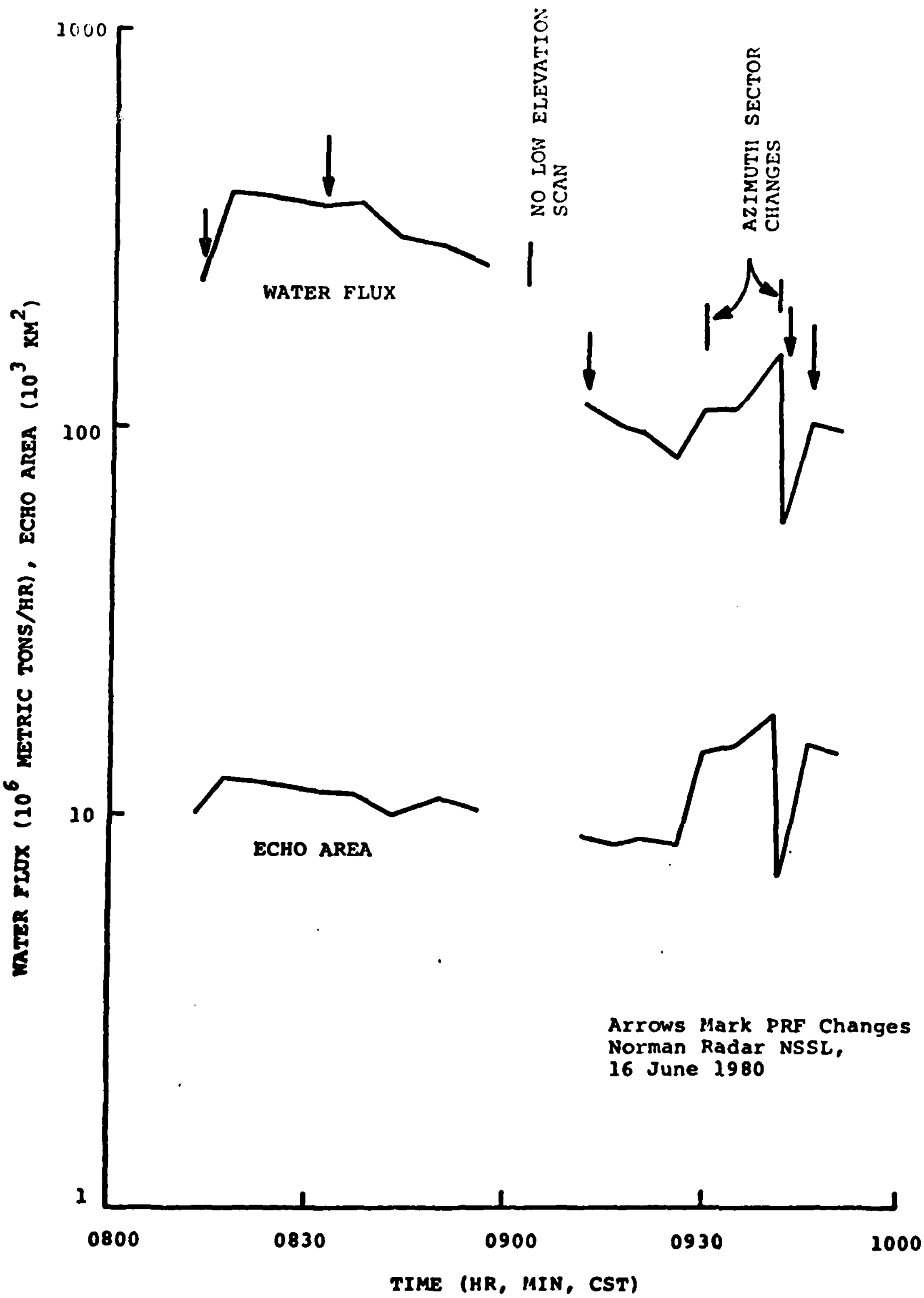

FIGURE 12. Summary parameters for the June 16, 1980 observation set. Both echo area and the water flux (area integrated rain rate) are displayed.

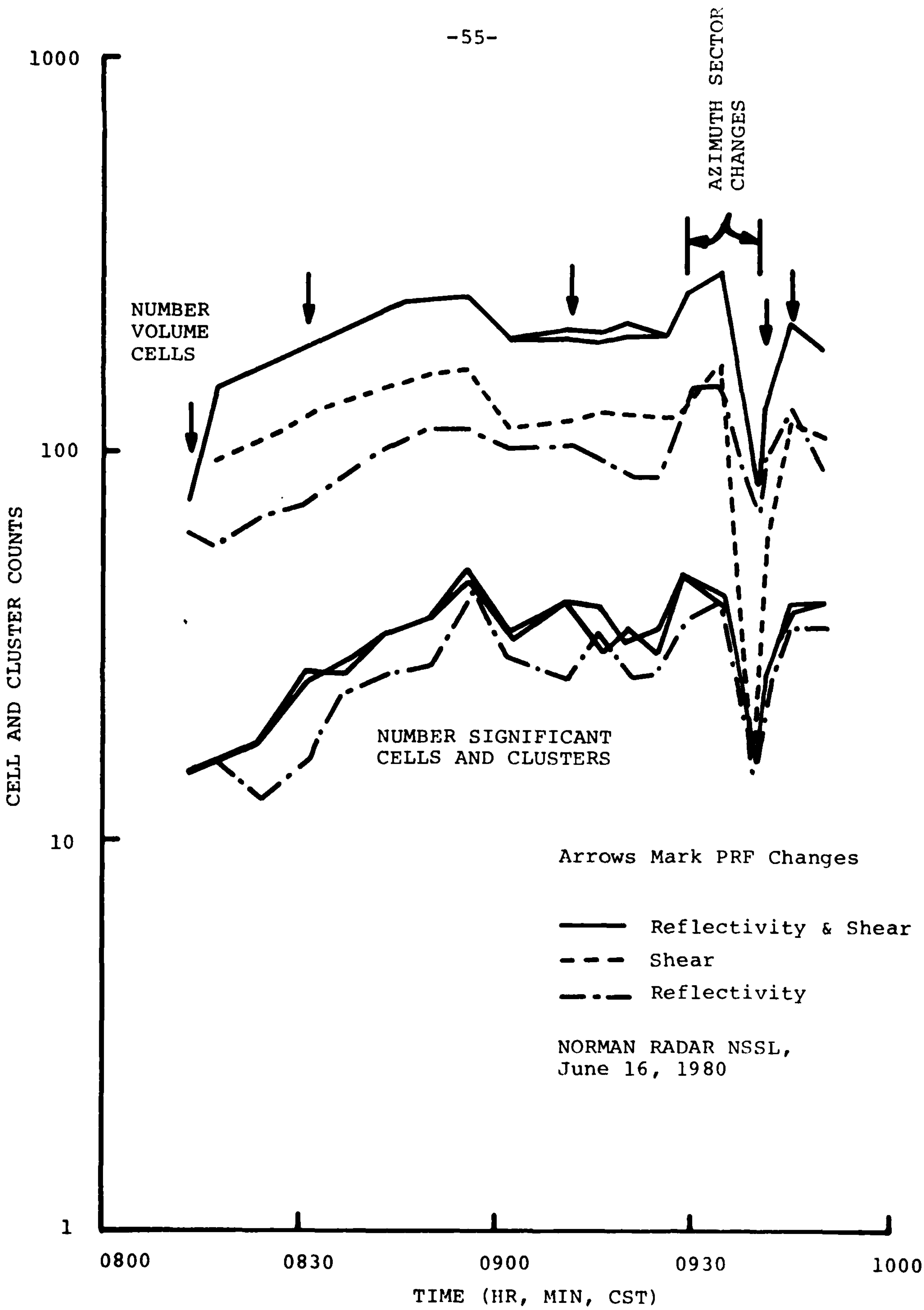

<u>**FIGURE 13**</u>. Counts of the numbers of active volume cells and clusters for four separate tracking runs.

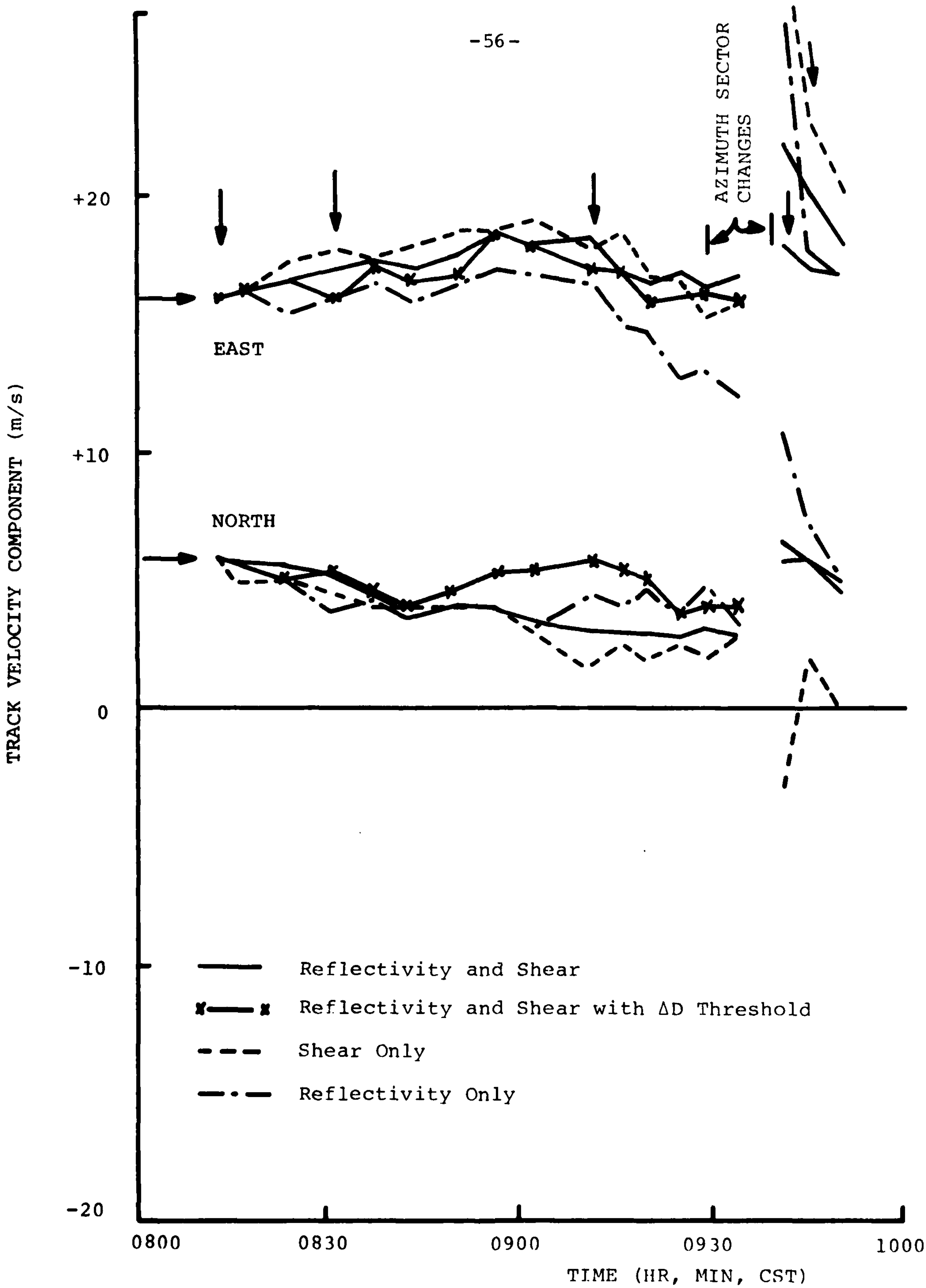

FIGURE 14. Average tracking velocities for the separate tracking runs.

smallest tracking error (Figure 15) but used less than 20 percent of the volume cells for tracking (Figure 16). The restricted tracking procedure could not cope with the transient at 0940 caused by an extremely short scan sequence, an adjustment in the sector boundary, and a change in the radar parameters. The times for parameter (prf) changes are noted by arrows on each of the figures.

The tracking algorithm was revised to associate more than one velocity perturbation cell with a volume cell on each scan of a tilt sequence. New volume cells were declared if, for each velocity perturbation cell, no volume cell was available for association. The revised program did not use a velocity perturbation volume cell for tracking unless it had been observed twice. The revisions were made to reduce the false velocity perturbation problem encountered in the analysis of the NHRE case study data and to incorporate the time continuity requirement to effectively increase the number of samples used in detecting a velocity perturbation. Therefore, the numbers of volume cells, cells used for tracking and tracking errors are not displayed until the third volume scan. Since multiple velocity perturbation cell association is permitted, no clusters were detected when tracking was performed using velocity perturbation data only (run 3).

The total number of active volume cells was highest when

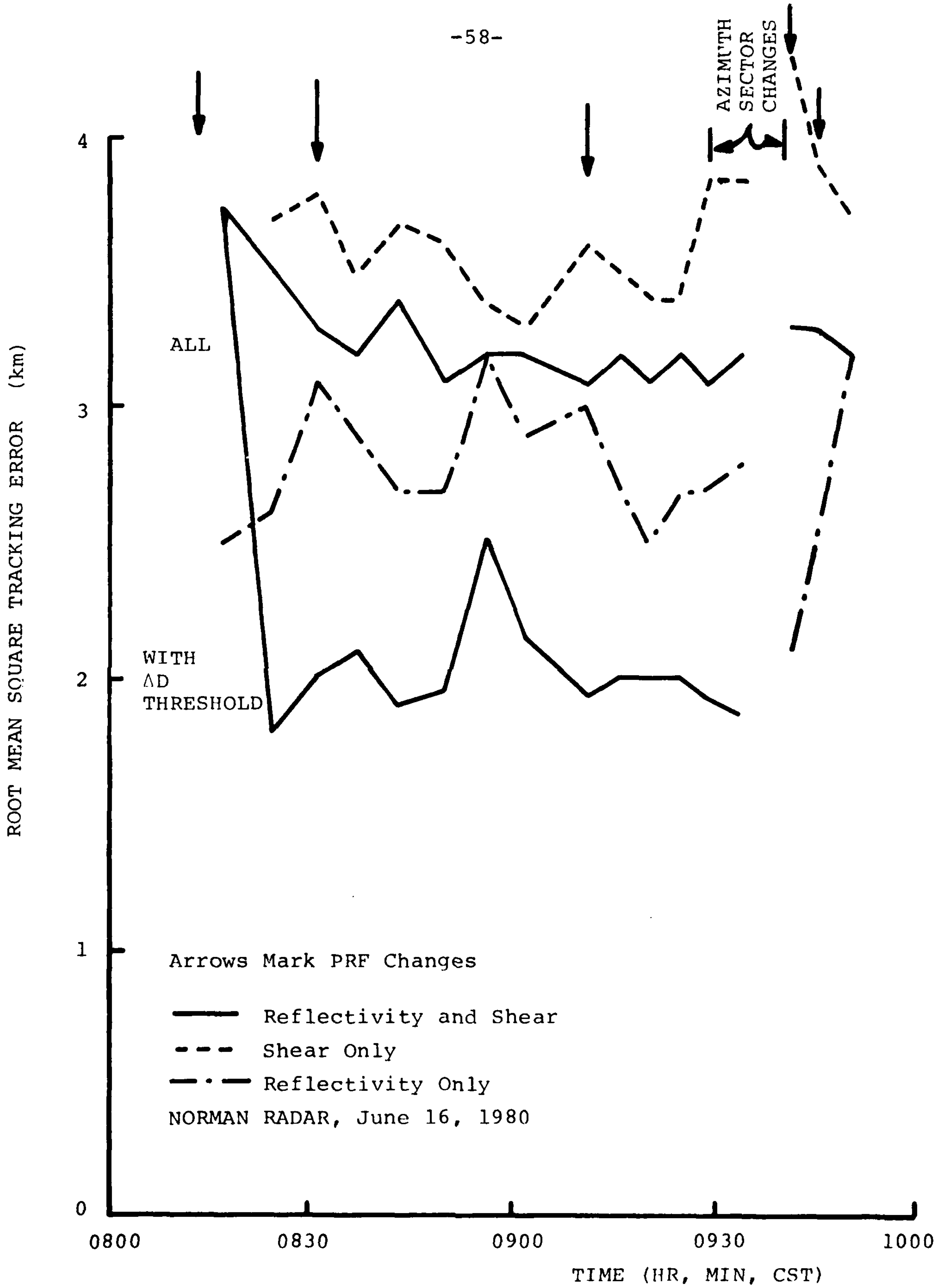

FIGURE 15. RMS tracking errors for the separate tracking runs.

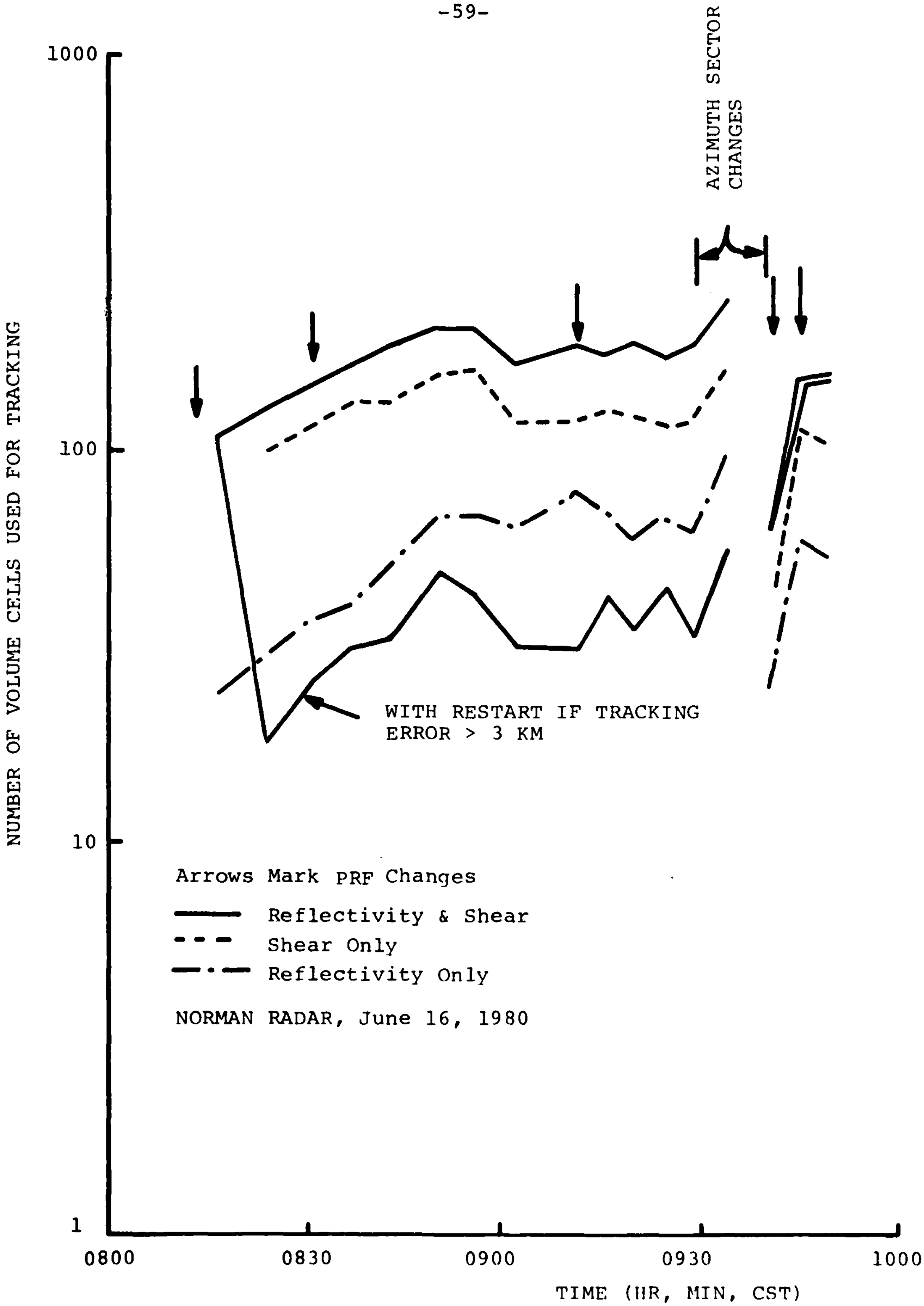

FIGURE 16. Number of volume cells employed for tracking in each of the tracking runs.

the reflectivity and velocity perturbation data were combined (Figure 13). The number of volume cells and detected significant cells and clusters were nearly identical for the two runs employing reflectivity and velocity data (runs 1 and 4). The small differences between the numbers of active cells and clusters for the two runs were produced by the differences in the smoothed track velocities used for initialization. The number of reflectivity only cells (run 2) was typically less than half the total number of cells and the sum of the number of velocity perturbation and cells and reflectivity only cells was roughly equal to the number of combined reflectivity plus velocity cells. These results indicate that the velocity perturbations were often remote from the reflectivity cells. The initial model assumed that the velocity perturbations would be associated with the reflectivity cells and the addition of the velocity data would not significantly change the number of active volume cells.

Although the number of active volume cells more than doubled when the velocity perturbation information was included, the number of significant cells and clusters did not. This last result indicates that the velocity perturbations were in reasonably close proximity to the reflectivity cells because the combination of volume cells derived from the velocity perturbations and volume cells obtained from the reflectivity data did not significantly increase the spatial sizes and numbers of clusters.

The typical separations between reflectivity cells and velocity perturbations were longer than the 5 km maximum separation between the predicted volume cell and observed cell locations allowed for cell, volume cell association but close enough to suppress the detection of large clusters. In this combined data set, the largest cluster observed had a scale (largest horizontal distance) or less than 18.2 km. For comparison, the largest cluster (reflectivity only) found in this data set had a scale of 16.8 km and in the NHRE data set had a maximum linear dimension of 18 km. The NOAA-C Doppler radar identified significantly larger clusters with the processing algorithm used in the prior study. The new processing algorithms therefore were successful in protecting against excessively large clusters in the presence of a large number of velocity perturbation cells.

The median root mean square tracking errors (the root mean square differences between observed and predicted volume cell locations) after the initialization transients had passed, were largest for the velocity perturbation data only (3.5 km after stabilization), were smallest for the reflectivity data only (2.7 km) and were 3.2 km for the combined reflectivity plus shear data when no restriction was placed on the magnitude of the tracking error (except for the initial association restriction). It is noted that the rms tracking error for reflectivity data only is equal to the maximum resolution volume dimension, D_m, of the radar at the median range to the volume cells. If an additional restriction were used, smaller tracking errors were

evident (2 km) but less than 20 percent of the volume cells satisfied the restriction and were used in tracking. The smoothed track velocity did not adjust to changing conditions within the surveillance region (Figure 13), however, thus defeating the purpose of the adaptive adjustment of the velocity employed for track initiation. Note that the reported tracking velocities are in the directions of cell motion and not in the direction (meteorological) of a steering wind.

The study of the effectiveness of the tracking algorithm was undertaken to obtain information about tracking (and prediction) errors when velocity data are combined with reflectivity data and to evaluate the utility of obtaining rotation and divergence data from the relative locations of volume cells within a cluster. The latter information is of interest (1) for attempting to obtain hazard data from conventional radars (no Doppler data) and (2) for providing additional information for use in assaying the probability that a cluster and its associated velocity perturbation is hazardous for aircraft penetration. The attempt to reduce the tracking error was based on the assumption that large tracking errors produce large uncertainties in cluster rotation and divergence estimates. The tracking run with the restriction on the magnitude of the tracking error (run 4) reduced the number of cells tracked from one scan to the next so drastically that rotation and divergence estimates could not be made.

Cluster rotation and divergence estimates could only be made using reflectivity plus velocity data with no restrictions (run 1) and reflectivity data only (run 2). After the tracking transient at 0940 the track reset was not activated (the

tracking errors were too large) and comparison could be made for both reflectivity and velocity data from the last volume scan but with different track initiation velocities. Two types of comparisons were possible, between the average tangential shear for a cluster and its rotation estimate (Figure 17) or its divergence estimate (Figure 18), and between the rotation or diversity estimates for reflectivity plus velocity perturbation data vs. the same estimates for the same clusters with different initialization velocities (Figure 19) or for the same clusters using reflectivity data only (Figure 20).

The data show no significant relationship between either cluster rotation (Figure 17) or cluster divergence (Figure 18) and tangential shear. Data contaminated by ground clutter are marked as are data obtained at ranges in excess of 150 km. Ground clutter is usually associated with large tangential shear estimates. The lack of correlation indicates that either additional information is being supplied by the cluster rotation and divergence estimates or that the tracking process is too noisy and the rotation and divergence estimates are meaningless. The intercomparison between cluster rotation estimates from different tracking runs shows a large spread (Figures 19 and 20) indicating that the tracking process is too noisy to obtain reliable cluster

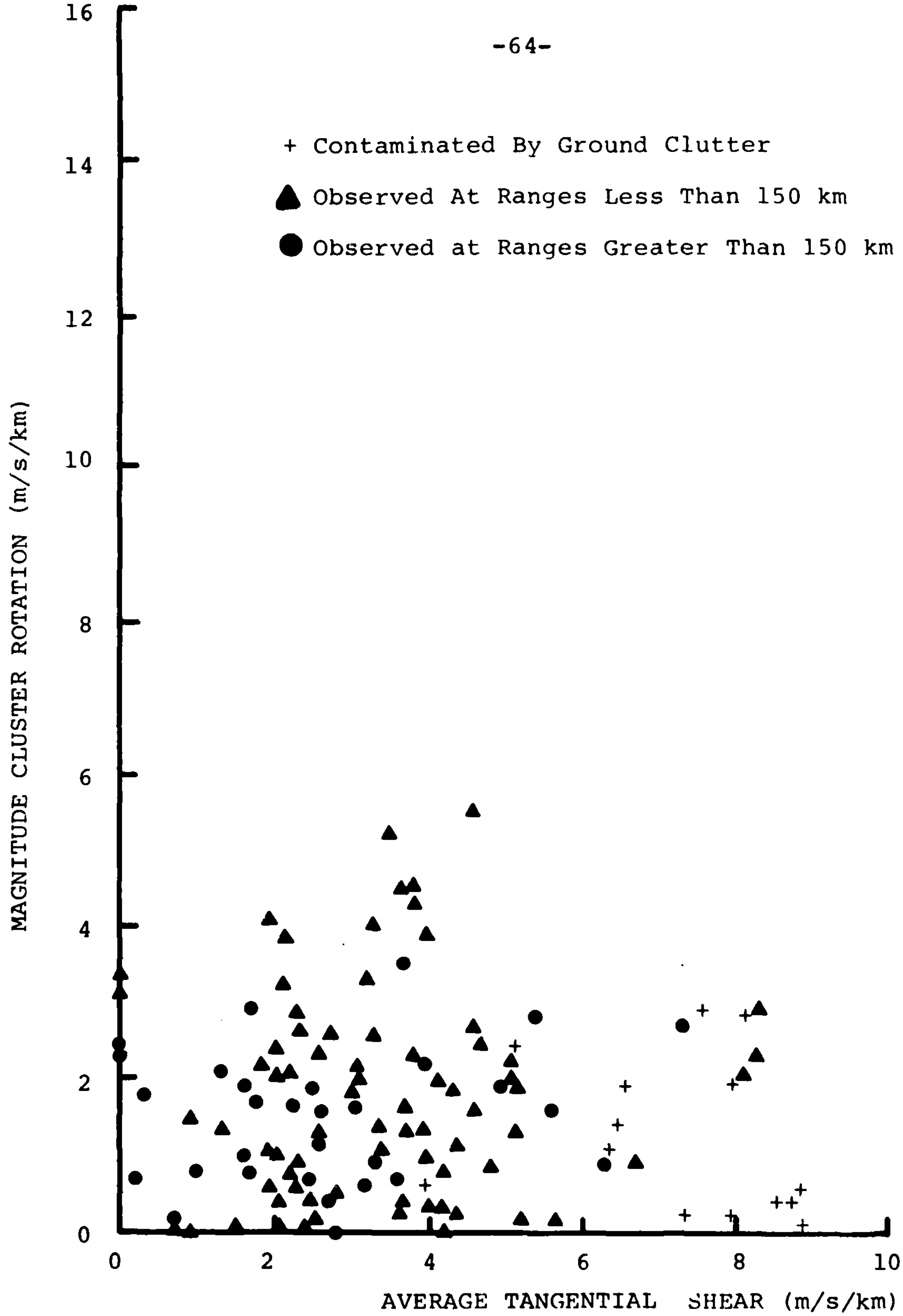

FIGURE 17. Rotation estimates for clusters based on tracking data.

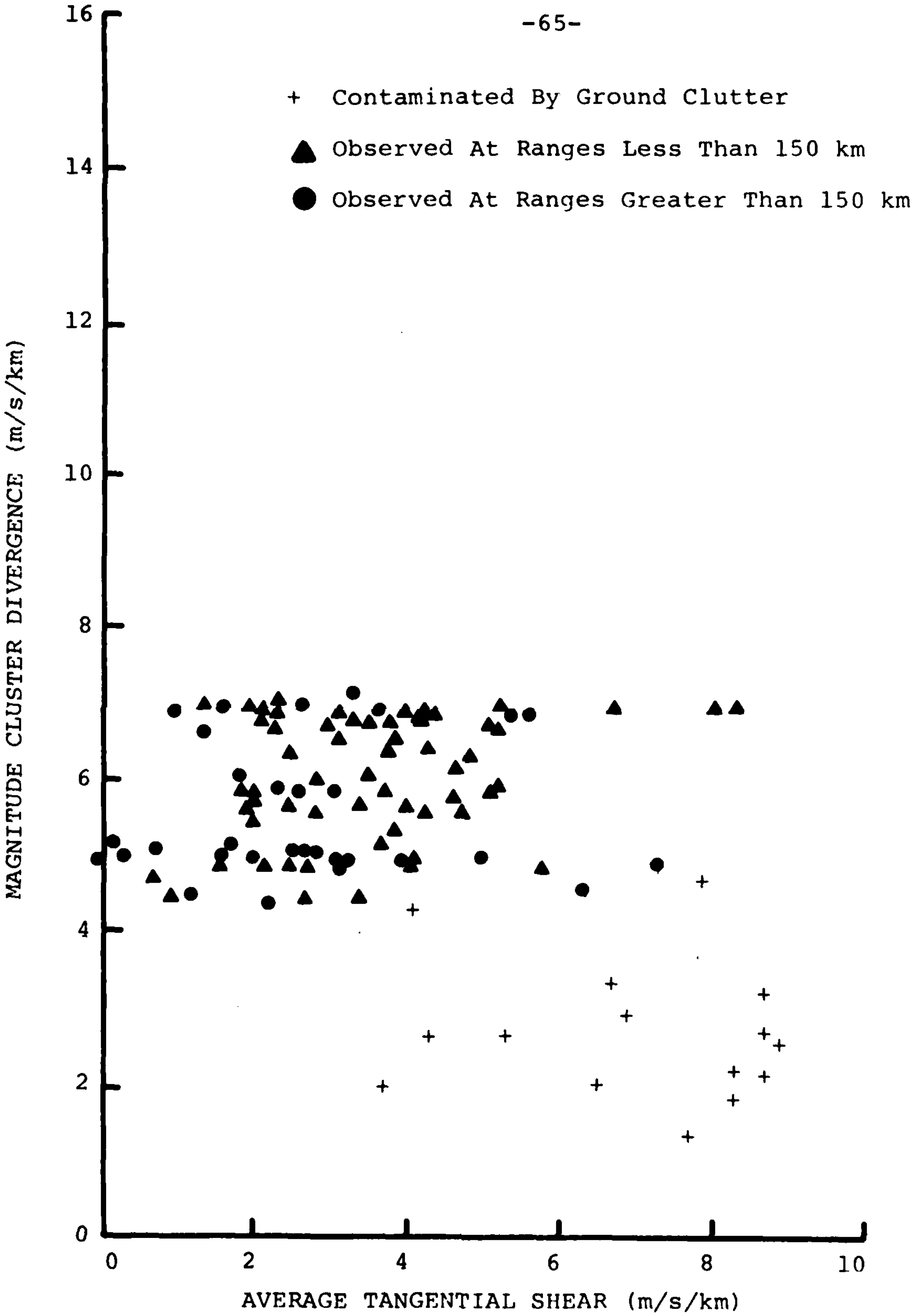

FIGURE 18. Divergence estimates for clusters based on tracking data.

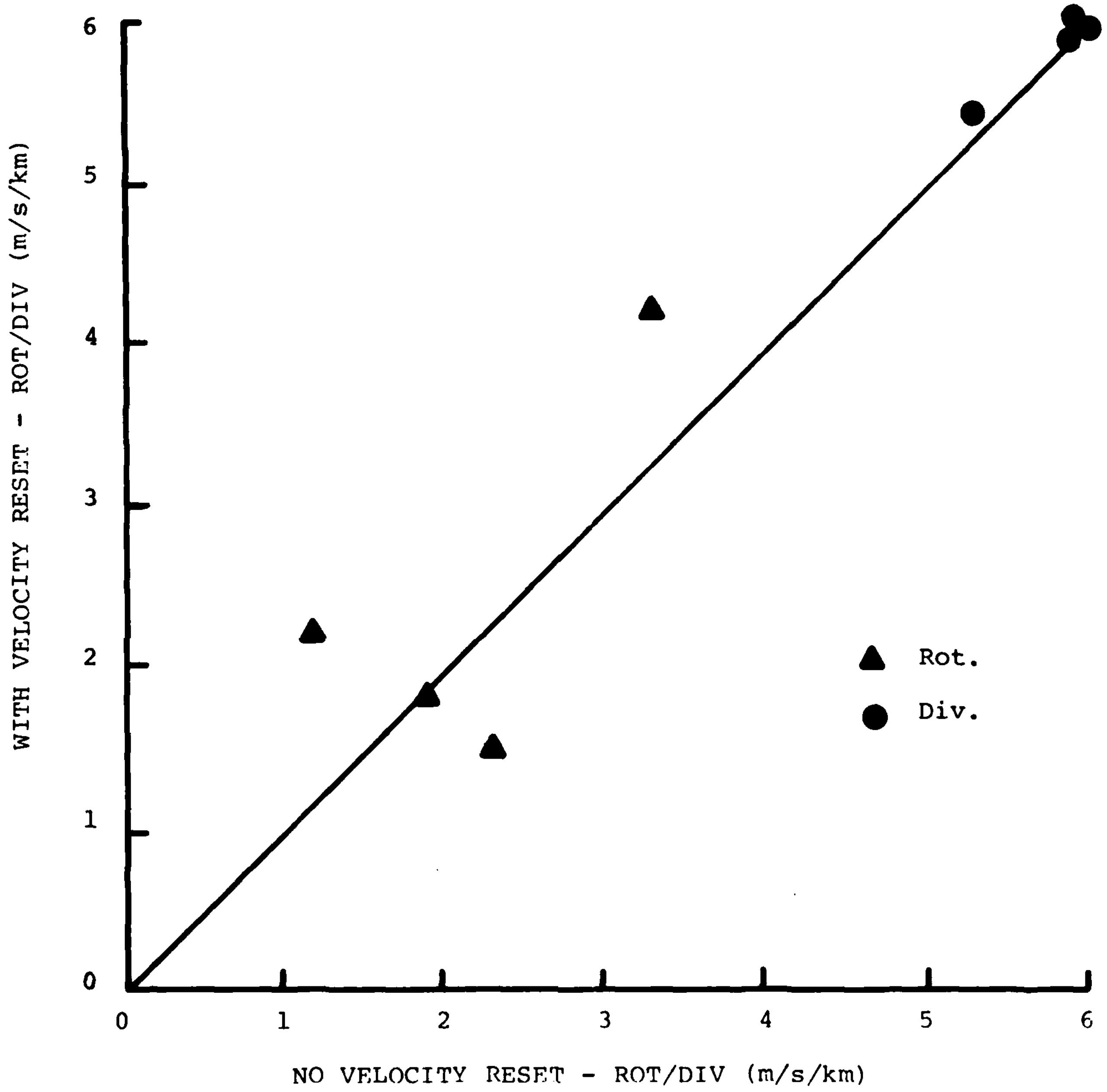

FIGURE 19. Comparison between rotation estimates and divergence estimates for identical data with different initial track velocity estimates.

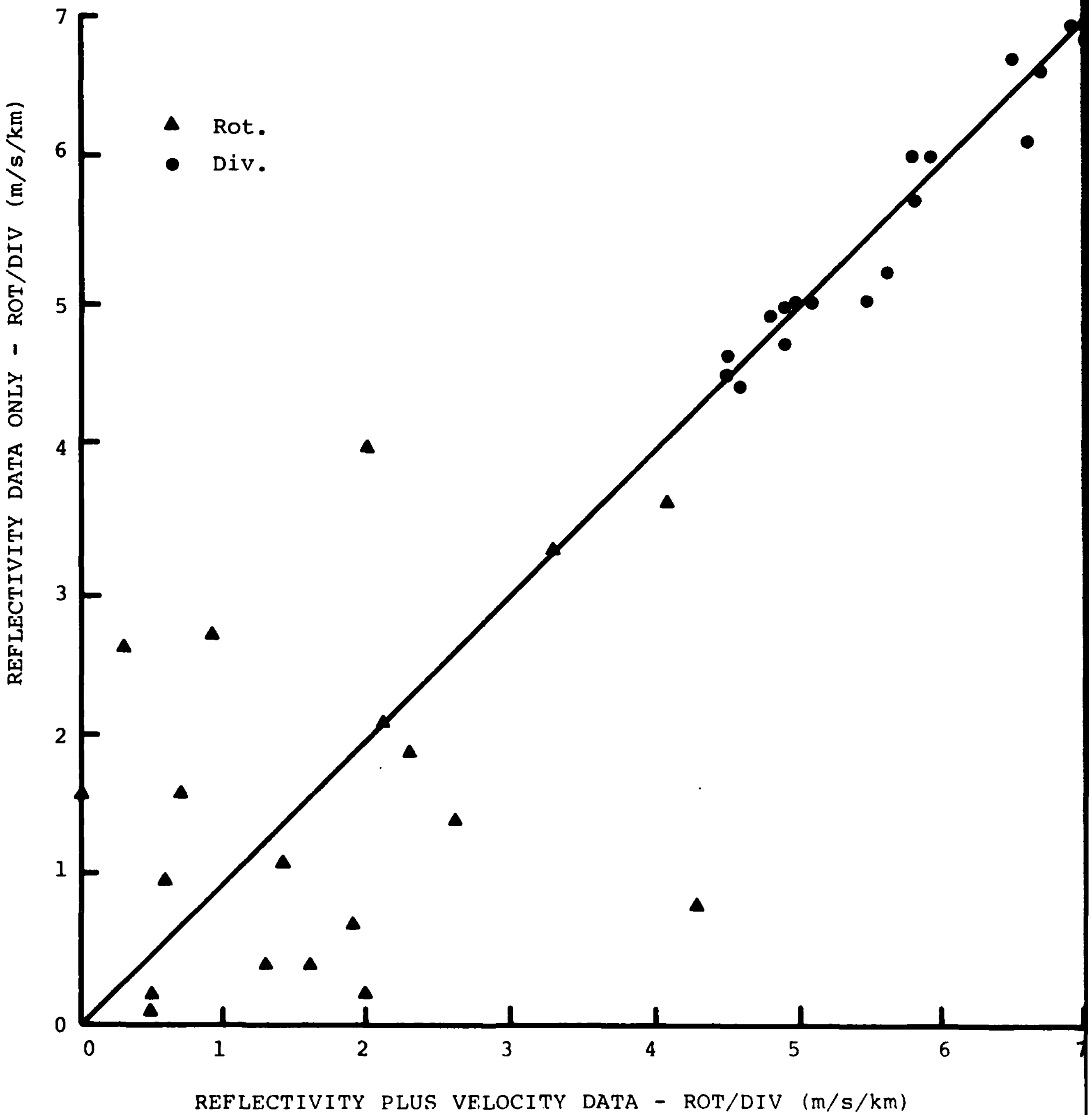

FIGURE 20. Comparison between rotation estimates and divergence estimates for the same clusters as detected using reflectivity data only or using reflectivity plus tangential shear data.

rotation estimates. The limited range of divergence estimates for a single volume scan suggests that although the cluster divergence data show good agreement between tracking runs 1 and 2 the results are not sensitive to the variations in the flow field that could represent variations in the potential for aircraft hazard.

The results of the tracking study show that tracks were successfully maintained on volume cells using either reflectivity only, velocity perturbation only, or both data types but that the tracking process was too noisy to allow reliable cluster rotation and divergence estimates. The false cluster detection problem has been solved but the use of reflectivity data only still produces the minimum tracking error. By associating a number of velocity perturbation cells with a single volume cell, the resulting tracking error was intermediate between using reflectivity data alone and velocity perturbation alone. The resulting position prediction error was less than 3.2 km rms, smaller than the radius of influence to be associated with a significant cell or cluster for hazard detection (Crane, 1981).

6. USE OF WSR-57 RADARS FOR HAZARD DETECTION

The prior study of turbulence hazard detection using weather radars showed that comparable results could be obtained using either conventional or Doppler radars. The promise of the Doppler radar is more information for use in reducing the false alarm problem. In the interim, before the availability of a network of Doppler radars, conventional radars may be successfully used for hazard detection. The question arises as to the suitability of the national network of National Weather Service (NWS) WSR-57 radars.

The cell detection process is built on the use of contouring algorithms. A cell is defined by a contour line that encloses all the radar resolution elements with reflectivity values within a fixed ratio of the peak value within the contour (conventional radar data). The cell location is the centroid of the enclosed resolution elements. Since the average area of a volume cell at the height of its peak value of reflectivity is only 5 km^2 (Crane and Hardy, 1981, Table 4-2), volume cells span only a limited number of resolution elements. For the Kansas data set, the average detected cell enclosed 4 resolution elements.

The Kansas data revealed a continuous decrease in cell detection probability with increasing observation range or

increasing cross-beam resolution distance (Figure 21). The range resolution of the Kansas Skywater 75, C-band, conventional weather radar was 1 km. When the maximum resolution element dimension, D_m, is 1 km, the average sized cell contains 5 resolution elements. The observed distribution of cell area is exponential(Crane and Hardy, 1981, Figure 4-4) indicating that more cells are smaller on the average than are larger. Cells of only one or two resolution elements are difficult to detect reliably leading to the observed change in detection probability with range.

The Kansas radar analysis program used data in the annular region from 25 to 150 km range. The behavior of the detection algorithm at shorter range (dotted curves) can only be inferred from the observations within the annulus. Two possible extrapolations are shown, (1) the linear extrapolation based on the exponential distribution size argument that some cells are too small to be detectable, and (2) the extrapolation using D_m (1 km at ranges shorter than 55 km) based on the argument that the relative frequency of occurrence should depend only on the relationship between cell size and D_m. Observations of all the volume cells detected in Kansas support the latter extrapolation curve while observations for volume cells tracked for 10 minutes or more support the former.

Extrapolation to larger D_m values is required to assay the

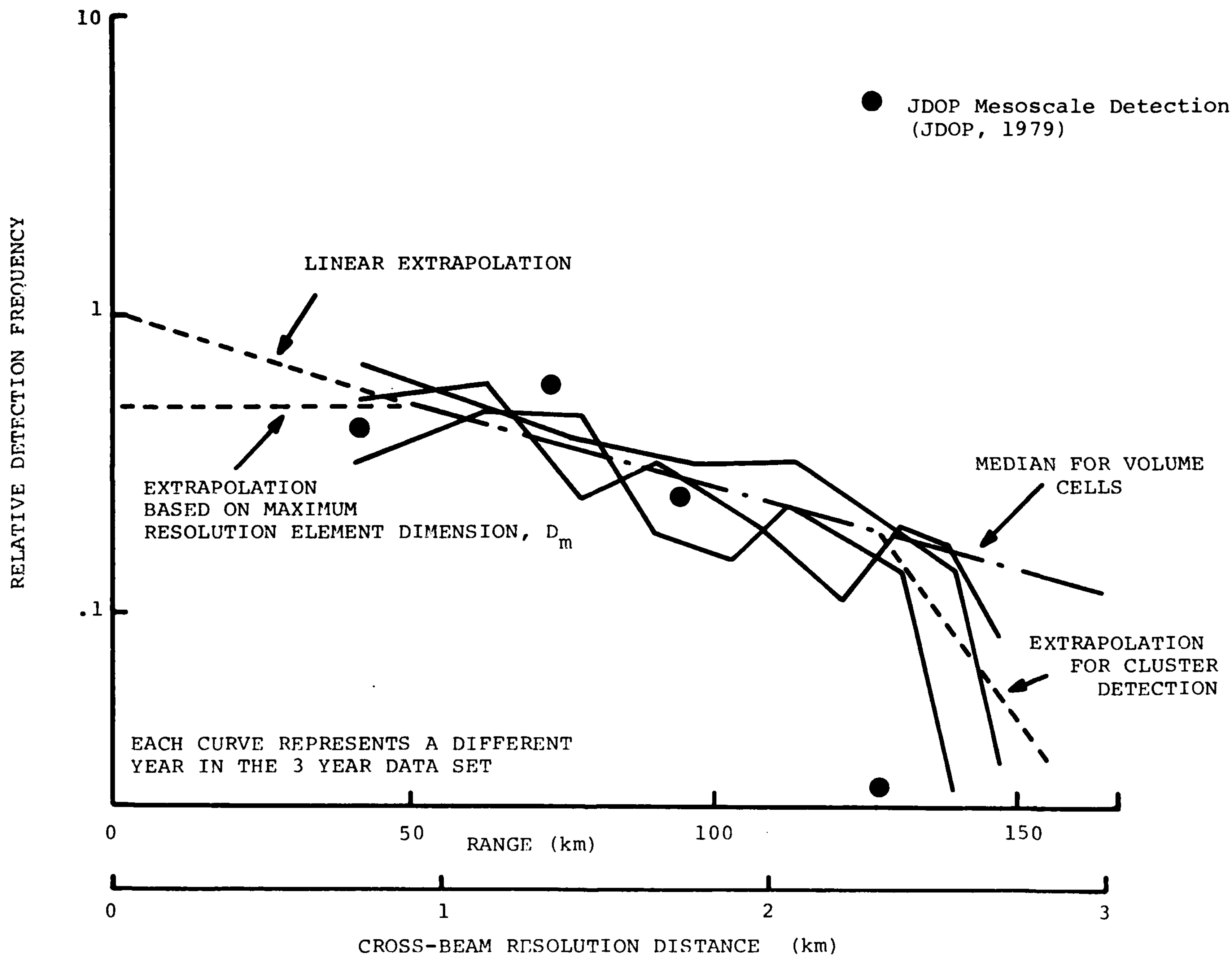

FIGURE 21. Relative detection frequencies for volume cells and clusters derived from the entire Kansas data set (Crane and Hardy, 1981, Figures 4-6).

utility of the WSR-57 radar because its beamwidth is more than double the beamwidth of the Skywater 75 radar or of the CP-2 radar implying D_m values more than twice as large at a given range.

Linear extrapolation to larger values of D_m is not possible because of the increased difficulty in detecting cells spanning only one resolution element. The analysis of the NHRE data showed that the ability to detect clusters was more important than the ability to detect single volume cells. Cluster detection requires the observation of 2 or more cells in close proximity. The average nearest neighbor distance between volume cells was 7 km for the Kansas data set (Crane and Hardy, 1981, Table 4-2). This corresponded to more than twice D_m at the longest range used for analysis and to roughly 6 times D_m at the median range for cluster detection. If the assumption is made that at least one resolution element is required between cells in a cluster for adequate cluster detection, then a change in the slope of the relative frequency for cluster detection should occur when D_m is 2.3 km (1/3 the nearest neighbor distance). A slope change is evident in Figure 21 as indicated approximately by the dotted curve labeled extrapolation for cluster detection.

Support for a slope change at a range near 130 km is obtained from an analysis of the variation in the number of mesocyclones detected as a function of range reported by JDOP

(1979, Part II Figures). The JDOP data are plotted on figure 21 as a function of range. The NSSL radars have one way half power beamwidth of 0.8°. Detection was accomplished using azimuth integration over 0.6° (dwell) with the integrator output sampled at 1° intervals. The effective half power beamwidth of the integrated radar data was less than 1° but, since samples were only available at one degree intervals, the data are equivalent to samples from a radar with a 1° beamwidth integrated and sampled every degree for the analysis of cluster or mesocyclone detection.

This analysis of the prior hazard detection study and the Kansas radar observations indicates that the WSR-57 should behave with capabilities equal to the CP-2 at half the range of the CP-2 radar. That is, for hazard detection, a 0.75 detection probability for moderate or more severe turbulence could be maintained to a range of 40 km. A rapid decrease in cluster detection probability will occur at ranges greater than 65 km suggesting that the utility of the radar will be limited for hazard detection employing the cluster observation algorithms at ranges larger than about 75 km.

7. INCORPORATION OF SATELLITE IMAGERY

The cell detection and tracking algorithms were developed for the observation and analysis of small spatial features of a scalar field such as reflectivity or tangential shear which persist for a number of observations of the field. Radar observations of the same cell may occur as rapidly as four times per minute or as infrequently as once per five minute volume scan depending upon the location and vertical development of the cell. Cell lifetime data indicate that the average lifetime is more than two volume scans and, for significant cells and clusters, the average lifetime is more than five volume scans. The data are sampled in time and space with sufficient resolution to associate cell occurrences from observation-to-observation and to provide tracks for the short range forecast of cell motion.

Geostationary satellite data are available which may be used to provide additional information for cell detection and tracking. The scanning visible frequency radiometer cloud data have a spatial resolution comparable to the resolution of a radar system but are not sampled frequently enough to allow automated feature tracking in the manner employed for radar cell tracking. The scanning infrared radiometer has a coarser spatial resolution but is still not sampled often enough for the spatially smoothed features to persist from one scan to the next.

A number of procedures are possible for combining the visible, infrared, and radar data. The satellite data may be spatially filtered (degraded) to the point where the features persist and may be tracked from one satellite observation to the next. The satellite processing system could then operate independently of the radar data. A variation on this scheme would be to degrade the poorer resolution infrared data to provide larger scale trackable features and to use the visible imagery at its highest resolution to detect features such as overshooting tops. The smoothed infrared radiance data would be nonlinearly transformed to a convenient temperature (height) scale, quantized, and passed through the cell detection and tracking program. The higher resolution visible data would be transformed to a convenient brightness scale, quantized, and operated on by the cell detection program to obtain features such as isolated overshooting tops and clusters of such features. These features plus the radar data could then be associated with the infrared tracks. This processing scheme could be used to process the satellite data but would not provide the additional data needed for hazard detection on scales comparable to those provided by the radar.

The problem which could benefit from the use of combined radar data and satellite imagery is the detection of potentially hazardous regions in the weaker echo regions of

developing cells that may not be accessible to observation by the radar. For this problem, the basic storm structure observation, cell detection, and tracking would be conducted using the radar data. The visible and infrared cloud imagery would be processed at the highest possible resolution to provide information about new cloud development. Processing using nonlinear transformation, quantization, thresholding (brightness and effective height) and subsequent cell detection would put the satellite data into a form which could be utilized by the tracking program. The satellite provided new cell development information would be associated with the translated positions of new radar cell development patterns to improve short range hazard forecasts.

The latter scheme for combining radar and satellite data was tried manually using radar data from Goodland, Kansas for August 24, 1977 and National Environmental Satellite Service (NESS) provided high resolution visible and infrared imagery at one hour intervals. At the early stages of radar cell development, the same features could be identified in each of the data sets. The visible data provided the best information on the location of cloud areas and fine cloud lines that later developed into more active convection. However, the data were not as useful as could be desired because the time of most active convection on the test day occurred after sunset when only the infrared data were available. The infrared data did provide useful information

about the location of a thin line of convective activity that later became detectable by the radar. The infrared data could not be used to locate regions of new cell development next to areas with active convection because of obscuration by cirrus clouds spreading from the active regions.

The satellite can provide additional information for combination with radar data. It is not a source of information that can be reliably used for hazard detection improvements in the weaker echo regions of new cell development because of the possibility of higher level cloud obscuration at the critical time. It would be very useful at the time of the initial development of the storm when the isolated, growing convective cells can be detected and their apparent growth rate and spatial organization can be observed.

8. CONCLUSIONS AND RECOMMENDATIONS

This report documents the development and testing of revised Doppler weather radar preprocessing, cell detection, and tracking algorithms which combine conventional radar reflectivity data and spatially filtered tangential shear data for the detection of volume cell clusters to be used for the location of turbulent regions hazardous for aircraft penetration. The revised algorithms successfully combine conventional and Doppler data without significantly increasing the number of detected volume cell clusters and without significantly increasing the tracking errors. The algorithms may be used to process conventional and Doppler data from a single radar or multiple radars in a weather radar network.

An analysis was performed which showed that the tangential shear data field and the Doppler spread (spectral width) data field contained essentially the same information for hazard detection for in-flight aircraft but the use of tangential shear was subject to fewer restrictions on the allowable signal-to-noise ratio. Additional spatial filtering and restrictions on the use of the Doppler data in the tracking routine was found to be necessary to further reduce the statistical uncertainties in shear (or spread) estimates and to reduce the number of false cell detections (false alarms).

The revised algorithms provide a number of new

attributes such as the vertical variation of radial velocity, cell age, ascent or descent of the average cell height during the initial stage of development, and incorporation in a cluster at the time of initial development which may be of use in refining hazard detection criteria. Although available, the use of the new attributes has not been explored due to a lack of aircraft penetration data for continued algorithm refinement and evaluation.

The algorithm refinement undertaken under this contract is a step toward the development of an automated, real-time hazard detection system for enroute and terminal area aircraft operations. Much remains to be done. In the conclusions and recommendations of the prior hazard detection study (Crane, 1981) a number of the remaining tasks were identified. They were repeated in section 2.1 of this report. They still need to be addressed.

Many of the tasks require the adjustment of parameters based on experience with a large data sample. Analysis to date has been based on an extremely limited data sample, a volume scan here, a 20 scan sequence on another day, two sets of penetration flights on two separate days, and 25 storm days of conventional radar data, with observations in the high plains of eastern Colorado, western Kansas and northern Oklahoma. The routine use of the detection and tracking algorithms on a significantly larger data set from a number of

different locations is required. The ultimate utility of these or any other weather radar processing algorithms will not be established until the have been tested on a large data set.

9. REFERENCES

Berger, T. and H. Groginsky, (1973), "Estimates of Spectral Moments of Pulse Trains", presented at the Int. Conf. on Information Theory, Tel Aviv, Israel.

Bohne, A.R., (1981), "Estimation of Turbulence Severity in Precipitation Measurements by Radar", Proc. 20th Radar Meteorology Conf., Amer. Meteorol. Soc., Boston, pp 446-453.

Crane, R.K., (1981), "Thunderstorm Turbulence Hazard Detection", ERT Doc P-2832-F, Environmental Research & Technology, Inc., Concord, MA.

Crane, R.K., (1980), "Radar Measurements of Wind at Kwajalein", Radio Science 15:383-394.

Crane, R.K., (1979), "Automatic Cell Detection and Tracking", IEEE Trans. Geoscience Elect. GE-17:250-262.

Crane, R.K. and K.R. Hardy, (1981), "The HIPLEX Program in Colby-Goodland, Kansas: 1976-1980", ERT Doc. P-1552-F, Environmental Research & Technology, Inc., Concord, MA.

Doviak, R.J., D.S. Zrnić, and D.S. Sirmans, (1979), "Doppler Weather Radar", Proc. IEEE 67:1522-1553.

Gustafson, G.B. and R.K. Crane, (1981), "Detection and Tracking Algorithm Refinement", DOT/FAA/RD-81/80, Federal Aviation Administration, Washington D.C.

Hjelmfelt, M.R., A.J. Heymsfield and R.J. Serafin, (1981), "Combined Radar and Aircraft Analysis of a Doppler Radar 'Black Hole' Region in an Oklahoma Squall Line", Proc. 20th Radar Meteorology Conf., Am. Meteorol. Soc., Boston, pp 66-70.

JDOP, (1979), "Final Report on the Joint Doppler Operational Project (JDOP)", NOAA Tech. Memo ERL-NSSL-86, National Severe Storms Laboratory, Norman, Oklahoma.

Lee, J.T., (1981), "Doppler Radar-Research and Application to Aviation Flight Safety, 1977-1979", Rept. DOT/FAA/RP-81/79, Federal Aviation Administration, Washington D.C.

Lee, J.T., (1977), "Application of Doppler Weather Radar to Turbulence Measurements which Affect Aircraft", Rept. FAA-RD-77-145, Federal Aviation Administration, Washington D.C.

Lee, J.T. and R.J. Doviak, (1981), "Field Program Operations-Turbulence and Gust Front Studies", Rept. DOT/FAA/RD-81/108, Federal Aviation Administration, Washington D.C.

Lewis, W., (1981), "Doppler Radar and Aircraft Measurements of Thunderstorm Turbulence", Preprints 20th Radar Meteorology Conf., Am. Meteorol. Soc., Boston, pp 440-445.

McCarthy, J., E.F. Blick, and R.R. Beusch, (1979), "Jet Transport Performance in Thunderstorm Wind Shear Conditions", NASA Contract Rept. 3207, Univ. of Oklahoma, Norman, Oklahoma.

Miller, K.S. and M.M. Rochwarger, (1972), "A Covariance Approach to Spectral Moment Estimation", IEEE Trans. Information Theory IT-18:588-596.

NCAR, (1982), "The JAWS Project, Field Operations Plan 1982", National Center for Atmospheric Research (NCAR) and Univ. of Chicago, Illinois.

Novick, L.R. and K.M. Glover, (1975), "Spectral Mean and Variance Estimation via Pulse Pair Processing", Preprints 16th Radar Meteorology Conf., Am. Meteorol. Soc., Boston, pp 1-5.

Waldteufel, P., (1976), "An Analysis of Weather Spectra Variance in a Tornadic Storm", NOAA Tech. Memo ERL NSSL-76, National Severe Storms Laboratory, Norman, Oklahoma.

Wilson, J., R. Carbone, H. Baynton, and R. Serafin, (1980), "Operational Application of Meteorological Doppler Radar", Bull. Amer. Meteorol. Soc. 16:1154-1168.

Zrnić, D.S., (1977), "Spectral Moment Estimates from Correlated Pulse Pairs", IEEE Trans. Aerospace Elect. Syst. AES-13:334-354.

Zrnić, D.S., (1982), Private communication.